DIEEI Sensor LAB
Dipartimento di Ingegneria Elettrica, Elettronica e Informatica

Open problems of utilizing noise in energy harvesting systems

B. Andò[1], S. Baglio[1], A. R. Bulsara[2], V. Marletta[1]

[1]*Department of Electric Electronic and Information Engineering, DIEEI, University of Catania*
bruno.ando@unict.it

[2]*Space and Naval Warfare Systems Center Pacific, San Diego, CA, USA*
bulsara@spawar.navy.mil

UPoN
GDAŃSK 2018

July 12th, 2018

DIEEI
University of Catania, Italy

Main activities of the Department are teaching, basic and applied research mainly focused on the following areas:

Information Technology
Automation, Control Systems and Robotics
Electro-technology
Electrical Systems
Electrical Machines, Drivers and Power
Electronics
Microelectronics
Instrumentation, Sensors and Multi-Sensor Systems
Telecommunication

Research Laboratories have been developed in areas above mentioned and each laboratory is equipped with up-to-date hardware and software systems both for the educational and the experimental activities.

DIEEI
University of Catania, Italy

Main activities of the Department are teaching, basic and applied research mainly focused on the following areas:

Information Technology
Automation, Control Systems and Robotics
Electro-technology
Electrical Systems
Electrical Machines, Drivers and Power
Electronics
Microelectronics
Instrumentation, Sensors and Multi-Sensor Systems
Telecommunication

Research Laboratories have been developed in areas above mentioned and each laboratory is equipped with up-to-date hardware and software systems both for the educational and the experimental activities.

RESEARCH ACTIVITY AT THE "SENSORLAB@DIEEI-University of Catania, Italy"

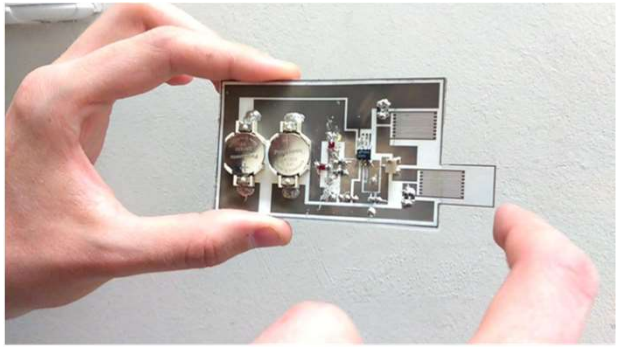

InkJet Printing sensing system

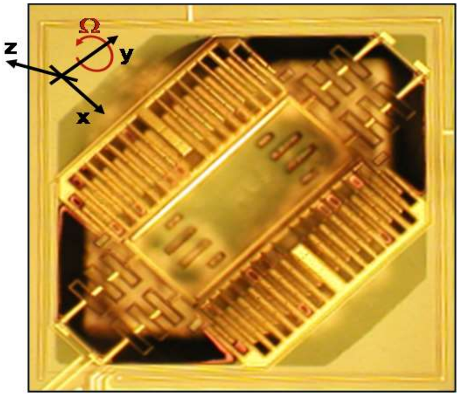

Microsensors

MAIN RESEARCH TOPICS

-Micro&Nano sensors
-Bio-sensors
-InkJet Printed Sensors
-Polymeric Sensors
-Ferrofluid based sensors

-Smart multi-sensor systems vs Applications (Assistive Technology, Autonomous sensing systems, monitoring of pollutions and seismic activity)

- Energy Harvesting

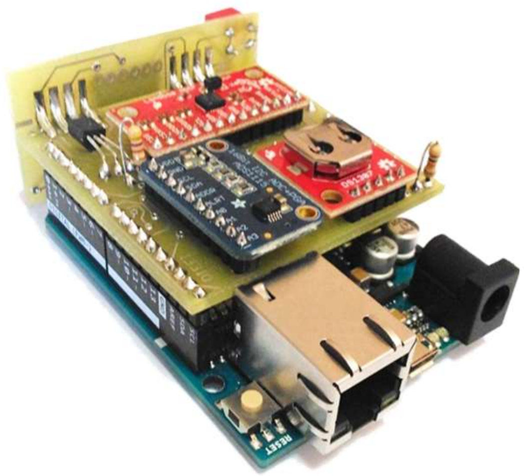

Embedded Multi-sensor Systems

Non Linear Energy Harvesting

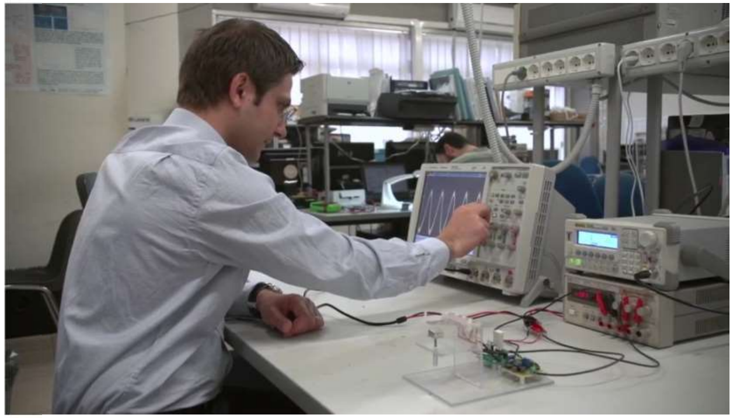

Sensor design, validation and characterization

Energy harvesting or scavenging is a process that captures small amounts of (unused) energy that would otherwise be lost as heat, light, sound, vibration or movement, to power small electronic and electrical devices making them self-sufficient (recharge/replace batteries).

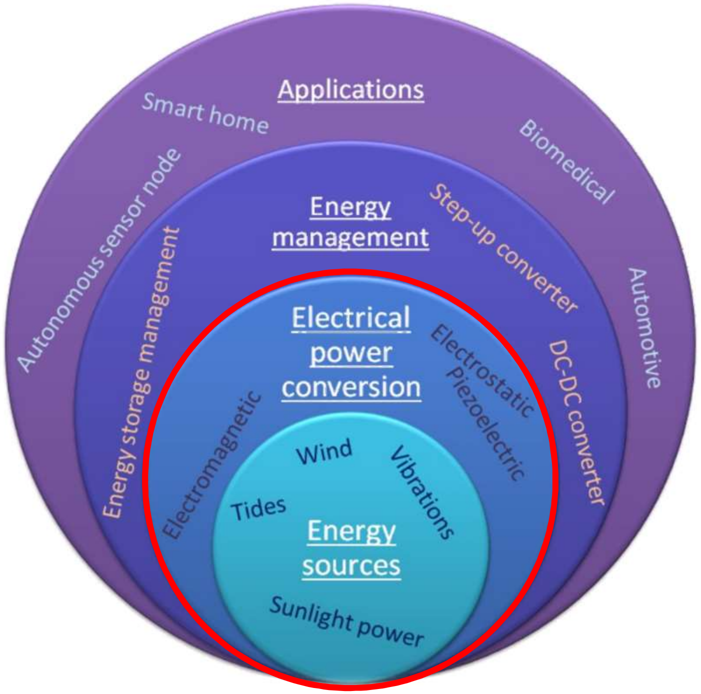

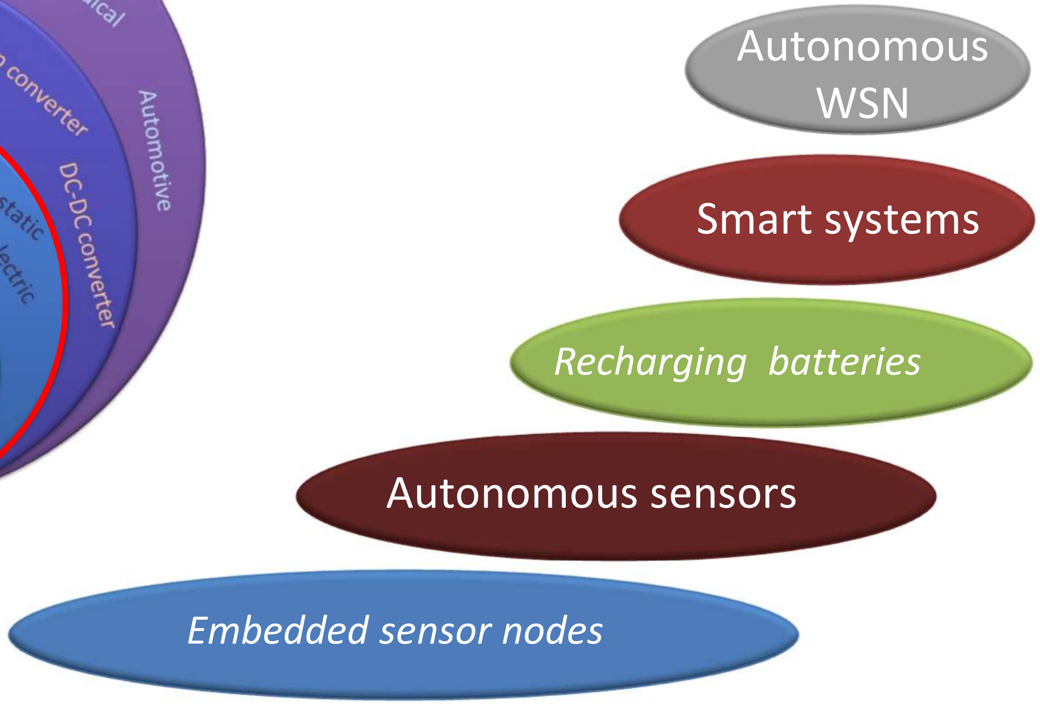

Benefits of EH

Maintenance free : no need to replace batteries

Improving efficiency: eg. computing costs would be cut significantly if waste energy were harvested and used to help power the computer

Enabling new technology: eg. wireless sensor networks (WSN) and smart dust

Opening up new applications: such as deploying sensors to monitor remote or underwater locations (hostile environments)

Environmentally friendly: disposal of batteries is tightly regulated because they contain chemicals and metals that are harmful to the environment and hazardous to human health

Wireless Sensor Nodes of WSNs

A WSN consists of:

- Sensors/Actuators
- Microcontroller (µC)
- Radio Tx-Rx
- Power (batteries, or…..)

Problems in Powering Wireless Sensor Nodes

- high power consumption of sensor nodes
- limitation of energy sources for sensor nodes:
- prohibitive cost of providing power through wired cables or replacing batteries
- Small devices are very limited in the amount of energy that the batteries can store
- Smart dust approaches make it impossible to battery replacement

Vibration Energy

Ambient vibrations come in a vast variety of forms:

Human activity

Home appliances

Cars

Machineries

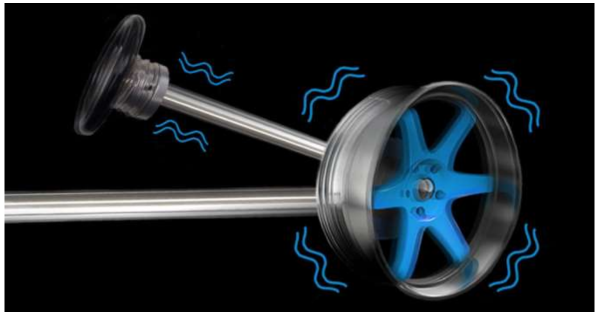

Ambient vibrations energy is distributed over a wide spectrum of frequencies.

•Piezoelectric materials *Mechanical stress ↔ electrical signal*

PM are ideal to collect Energy from Ambient Vibrations!

Human Walking- low-frequency vibrations are just some of the potential sources that could be harvested by piezoelectric materials

Human Actions – the force used to press a button of a remote control is sufficient to power a wireless radio or infrared signal

Human Motion – there is much interest in harvesting the kinetic energy generated by the footsteps of crowds to power ticket gates and display systems

Automotive – EH sensors attached inside the tyres continuously monitor the pressure and send the information to a display on the dashboard

•Thermoelectric materials *Temperature differences across the material ↔ Thermoelectric voltage*

A temperature across a thermoelectric crystal (i.e. one side is warmer/cooler than the other) causes a voltage across the crystal.

Road transport – Cars and lorries equipped with a thermoelectric generators (TEG) would have significant fuel savings.

•Pyroelectric materials *Change in temperature ↔ electric charge*

As the temperature of a pyroelectric crystal changes, it generates an electrical charge.

Pyroelectric EH

The pyroelectric effect is used in some sensors, but it is still some away from commercial energy harvesting applications

The general architecture of a Vibration Energy Harvesting system …

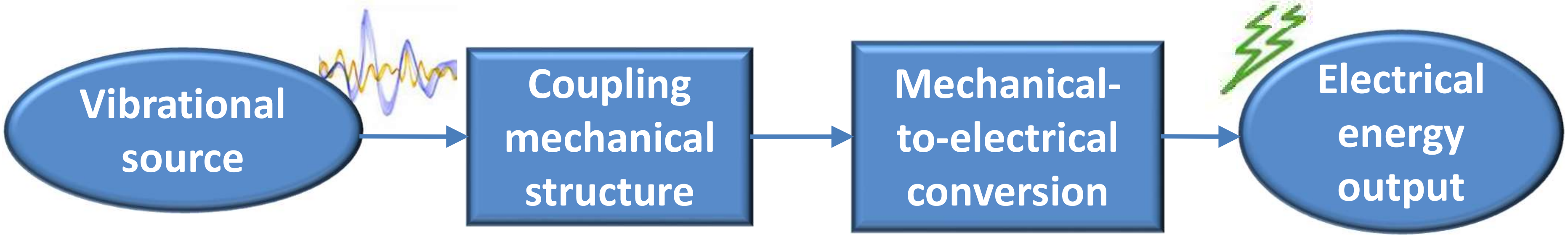

- Acceleration amplitude
- Frequency Spectrum
- …

- Linear
- Nonlinear
- …

- Piezoelectric
- Electrostatic
- Electromagnetic
- …

"Direct powering"
"batteries recharging" ?

LINEAR ENERGY HARVESTER & VIBRATIONS

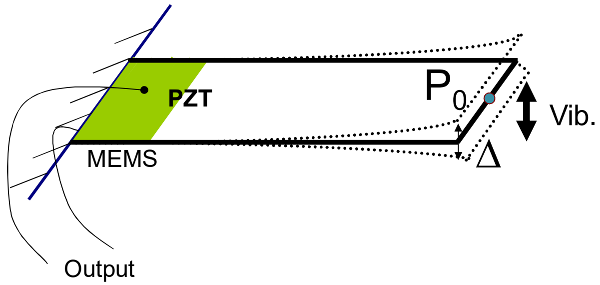

- Linear devices performs very well around their resonance frequency.
- Ambient vibrations come in a vast variety of forms, with an energy distributed over a wide spectrum of frequencies.

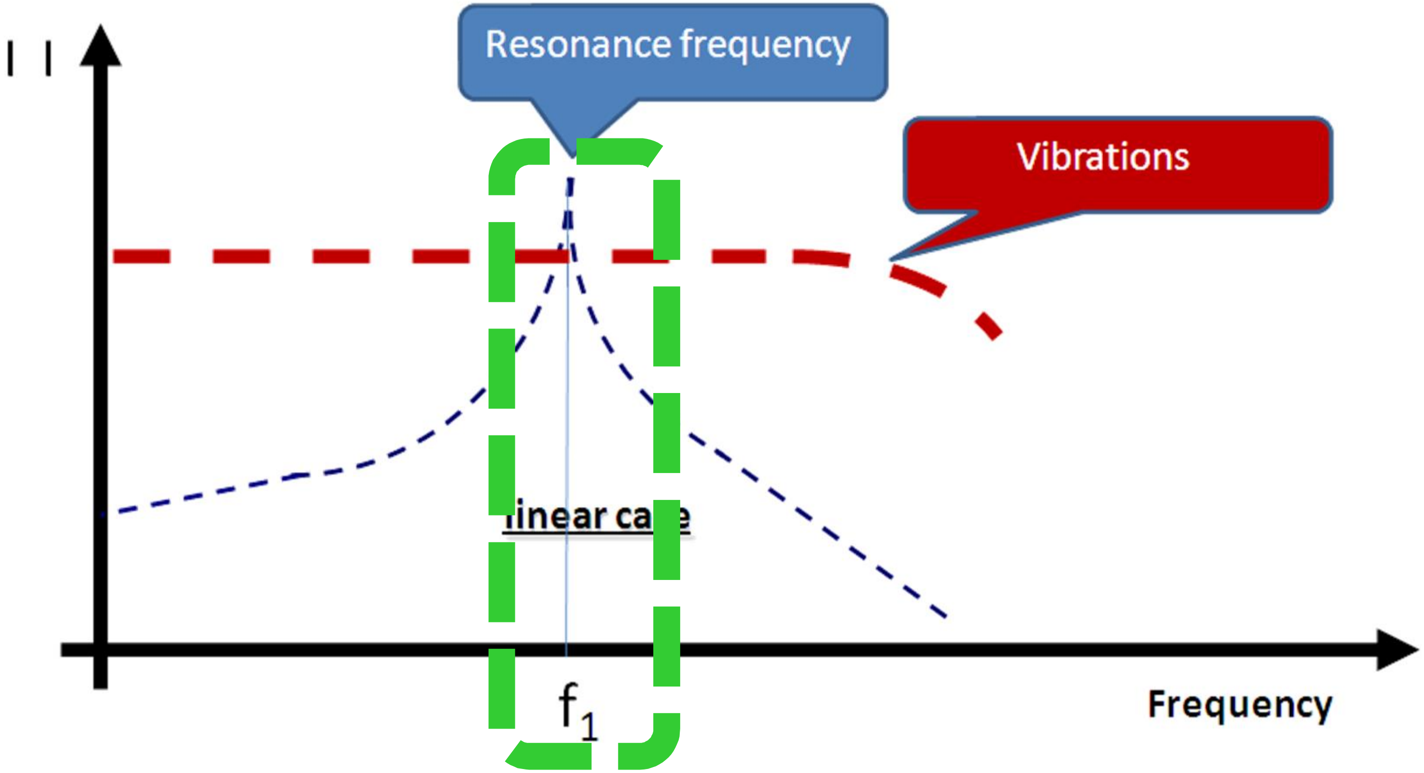

High efficiency around the natural frequency.

HOW TO INCREASE EFFICIENCY OF ENERGY HARVESTER?

Wish list for the 'optimal'' vibration harvester:

1) Harvesting energy over a wide frequency band
2) No need for frequency tuning
3) Harvesting energy below 100 Hz

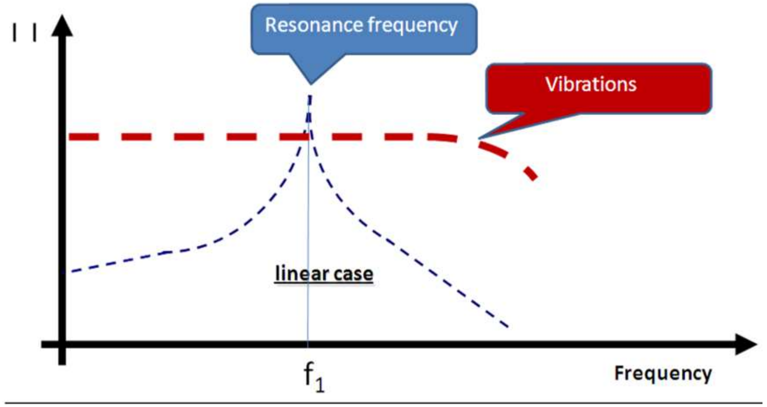

Several approaches have been proposed:

- Frequency Tuning
- Multi-modal devices
- Frequency up conversion mechanism
- Non Linear conversion mechanisms

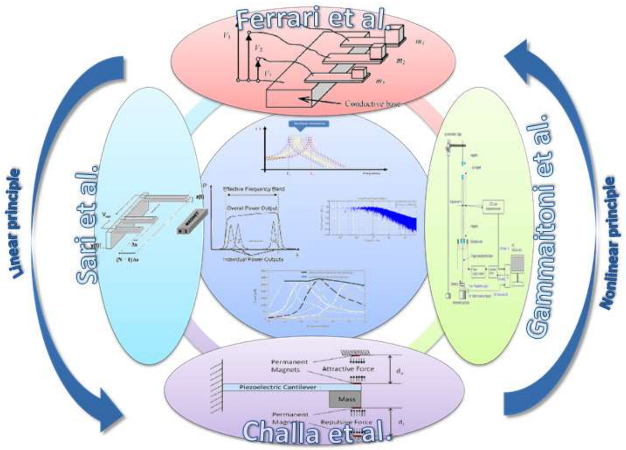

DIEEI – University of Catania, Italy

LINEAR HARVESTER vs NON LINEAR DEVICES

LINEAR HARVESTER

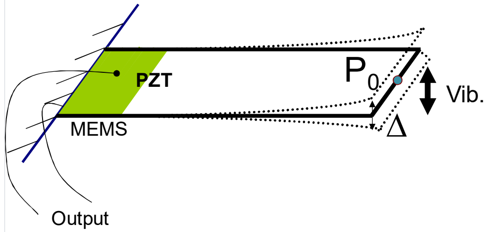

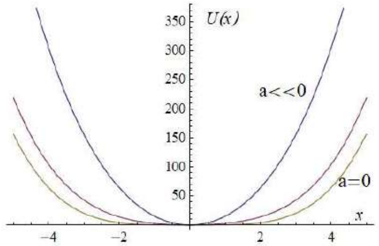

- Resonant behaviour
- Narrow frequency bandwidth
- Small inertial mass and high resonant frequency at micro/nano-scale
- Output power is a linear function of the input vibration

The Snap Through Buckling structure (STB)

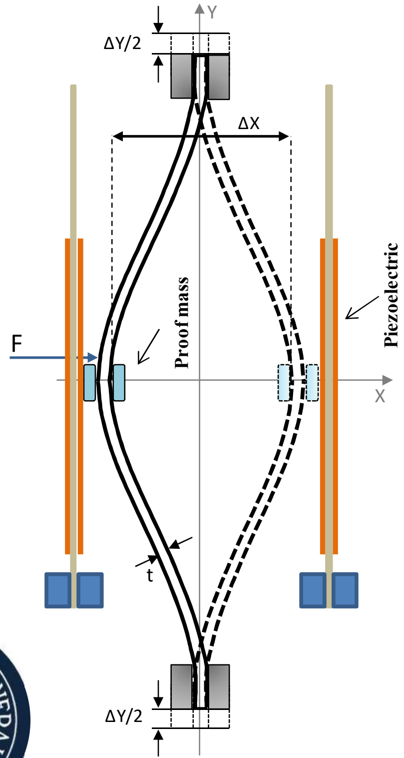

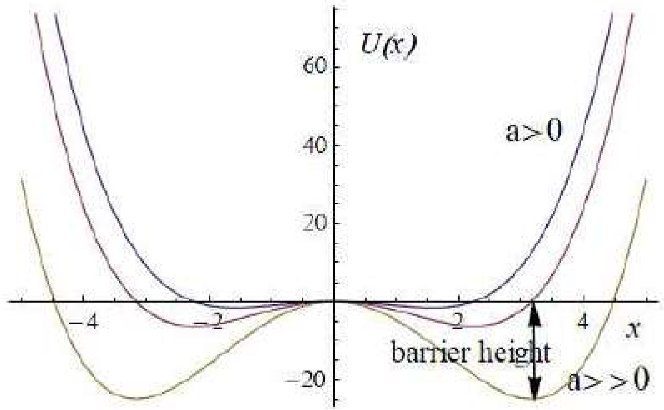

- Large frequency bandwidth
- Higher efficiency due to high impact velocity
- Increased beam strain
- Output power quite independent on the input strength

Non Linear Energy Harvester

@

Space and Naval Warfare Systems Center
Pacific, San Diego, CA, USA

ONRG - NICOP - N62909-15-1-2015 AWARD

THE DOUBLE PIEZO – SNAP THROUGH BUCKLING HARVESTER (DP-STB-NLH)

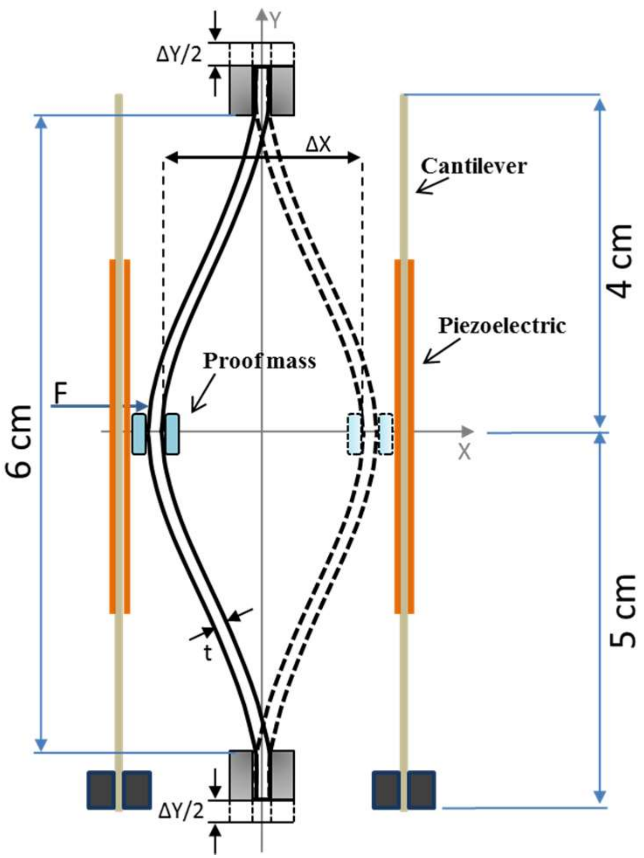

Schematization of the bistable nonlinear harvester

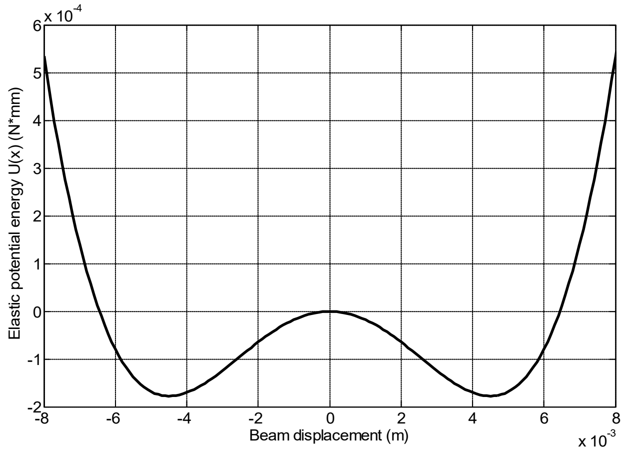

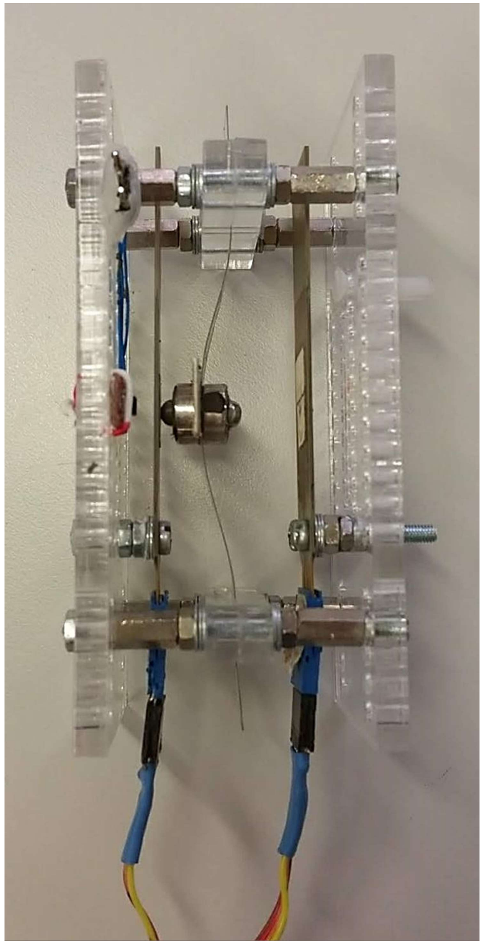

B. Andò, S. Baglio, A. R. Bulsara, V. Marletta, A. Pistorio, Performance Investigation of a Nonlinear Energy Harvester with Random Vibrations and Sub-Threshold Deterministic Signals, IEEE Trans. Instrum. Meas. 2017, 66(5), 992-1001.

THE PL-DP-STB-NLH

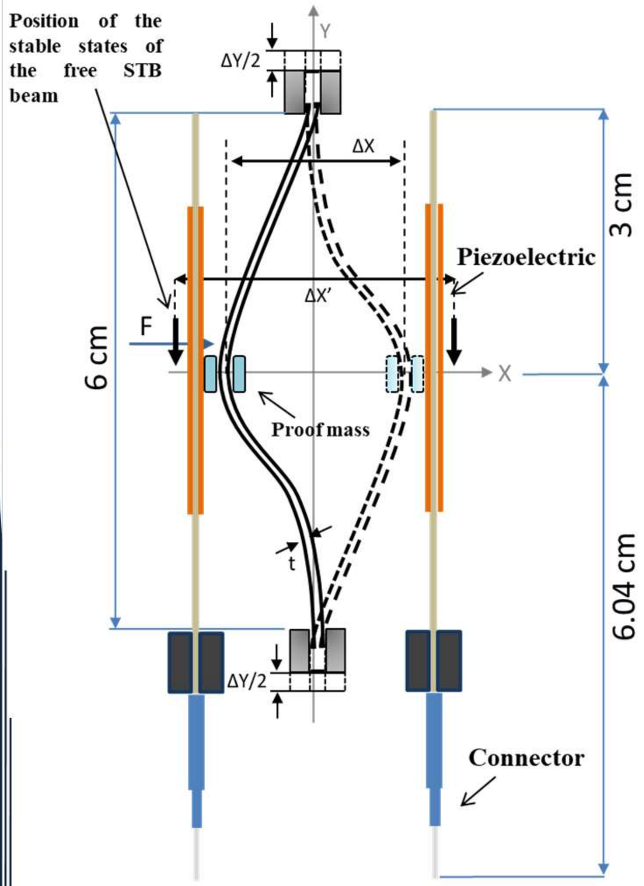

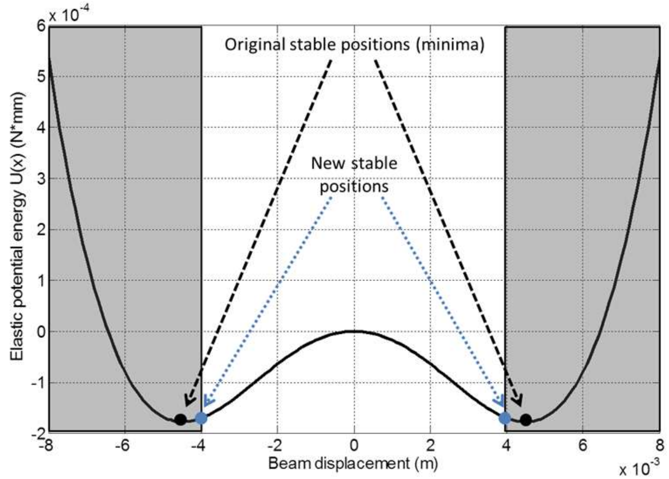

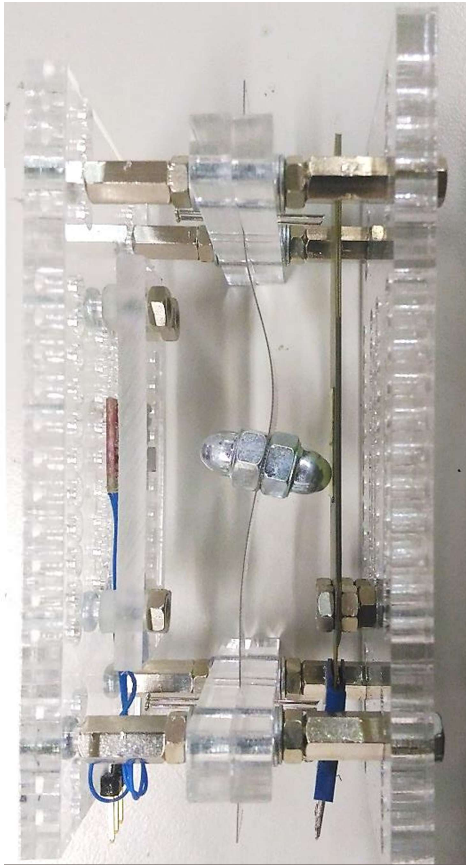

ΔY=1mm (precompression)
ΔX=7mm (distance between stable states)
PL= 1 mm (Pre-load)

B. Andò, S. Baglio, V. Marletta, A. Pistorio, A. R. Bulsara, A Low Threshold Bistable Device for Energy Scavenging from Wideband Mechanical Vibrations, accepted for publication on IEEE Trans. Instrum. Meas. 2018.

THE AR-DP-STB-NLH

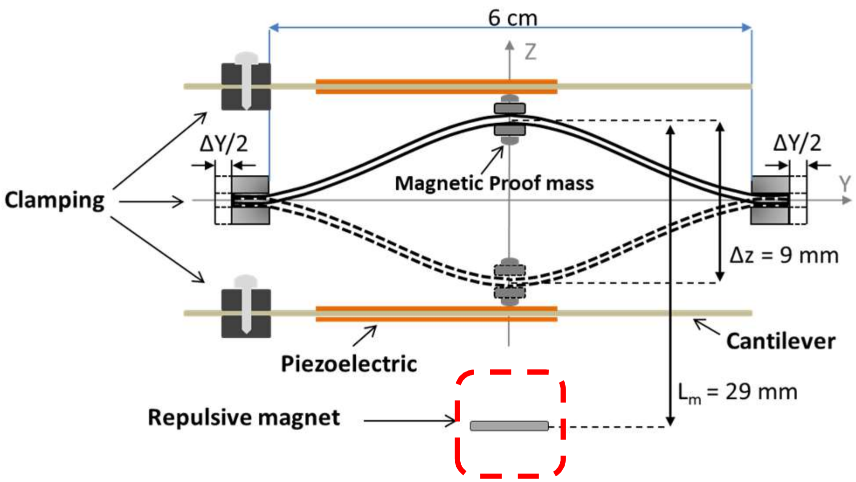

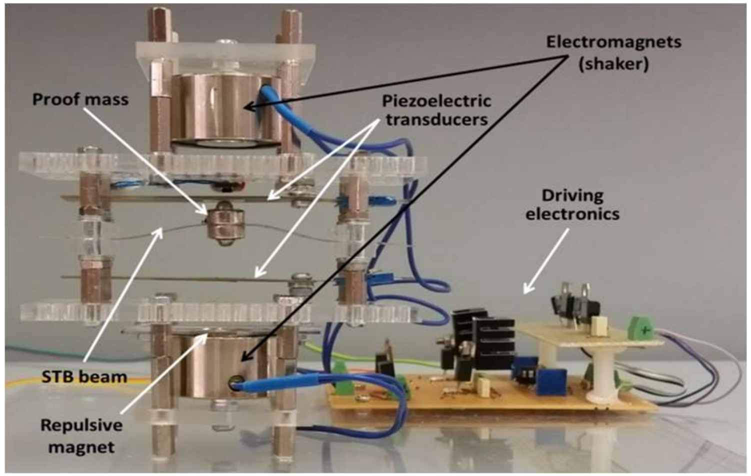

B. Andò, S. Baglio, V. Marletta, A. Pistorio, A. R. Bulsara, A Measurement Methodology for the Characterization of a Compensated Nonlinear Energy Harvester for Vertical Operation, accepted for publication on IEEE Trans. Instrum. Meas. 2018

How to estimate the optimal position of the repulsive magnet?

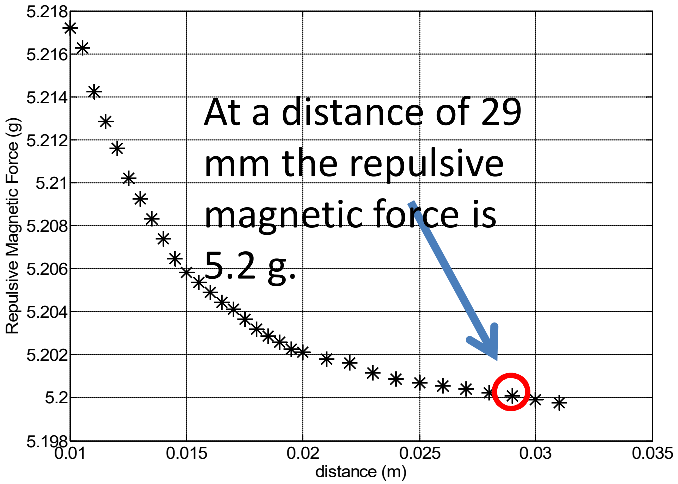

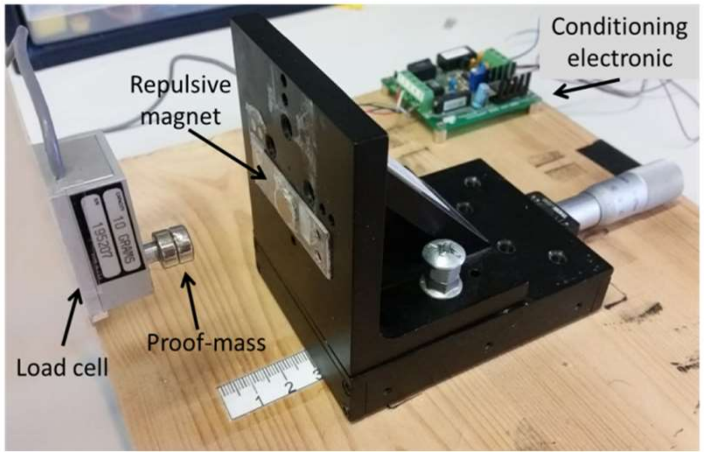

THE DP-STB-NLH: typical dynamics

2 Hz

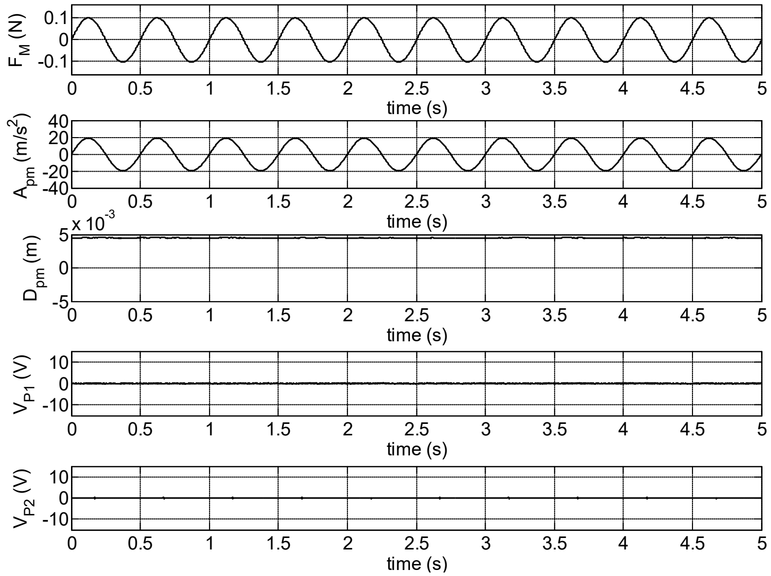

2 Hz

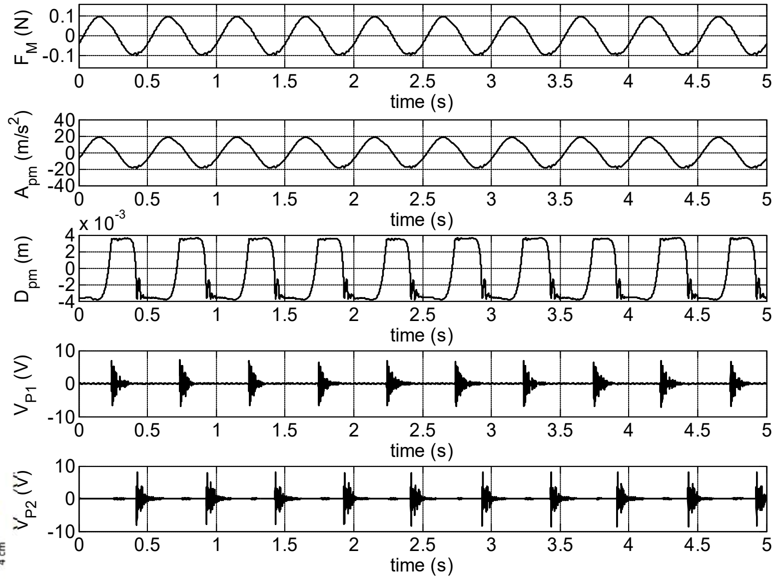

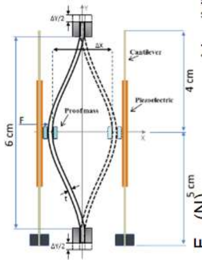

4 Hz

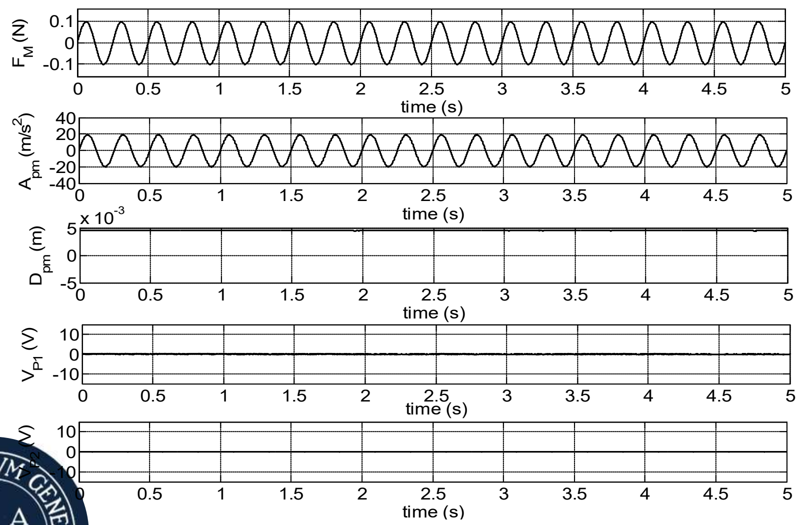

4 Hz

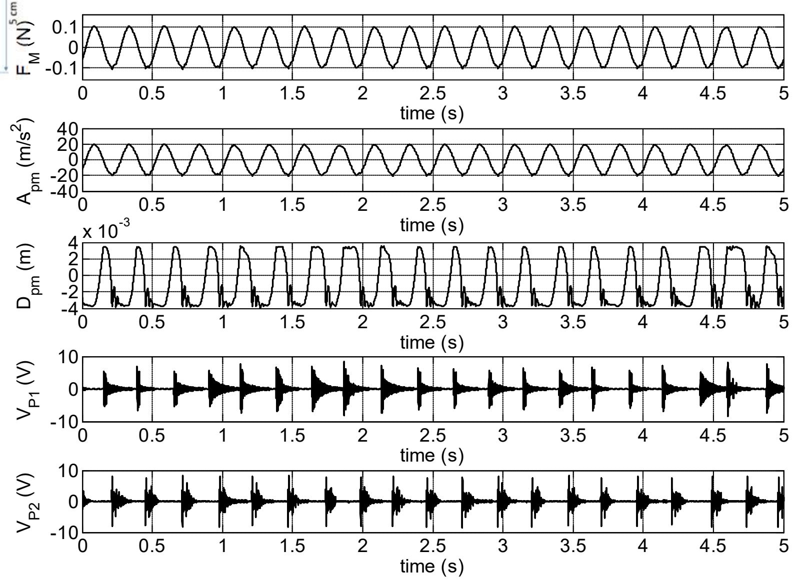

Behaviour in case of a Deterministic Input Signal

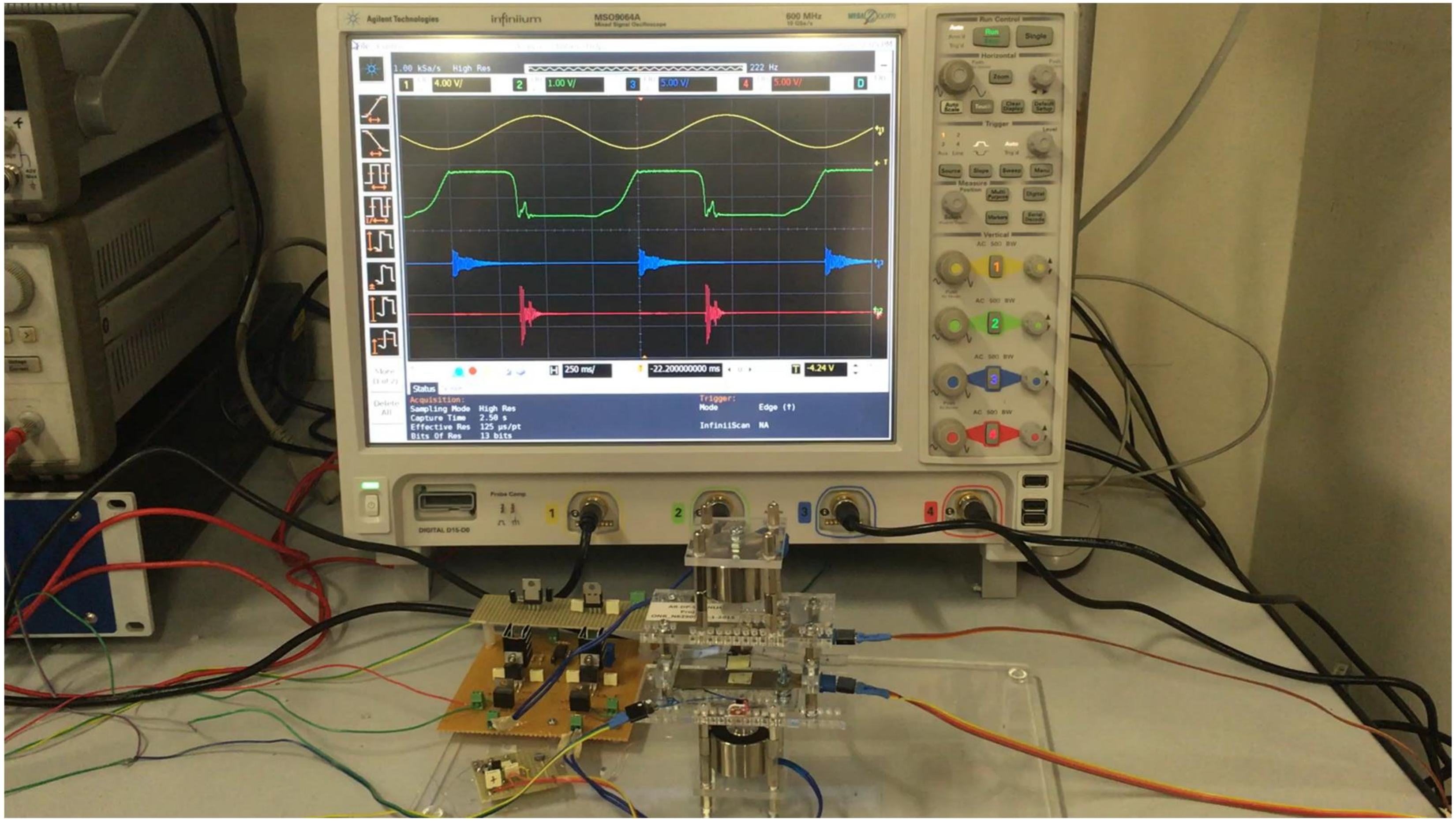

THE AR-DP-STB-NLH @ SensorLab - Unict

Performances in terms of number of swicthings

DP-STB-NLH

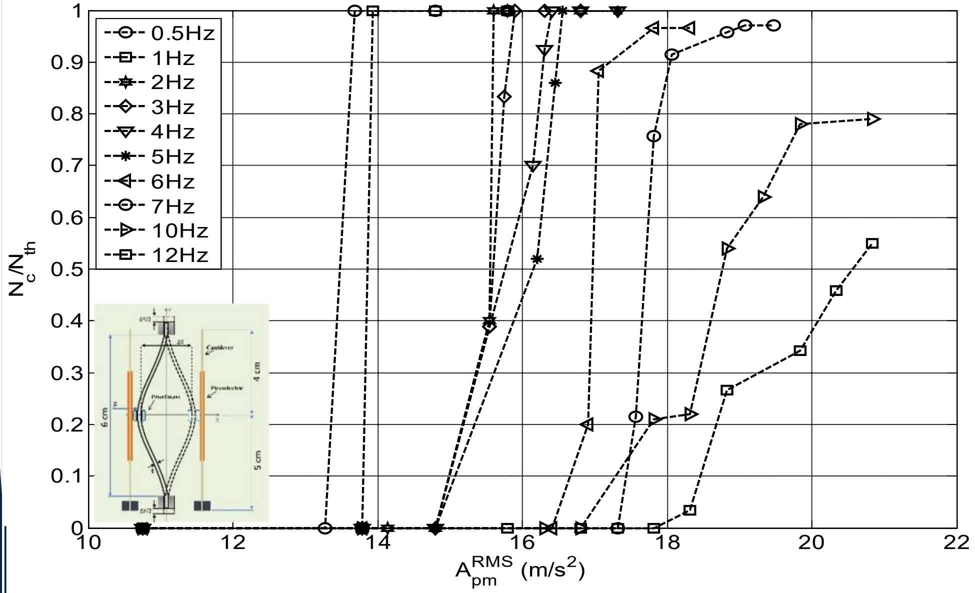

PL-STB-NLH

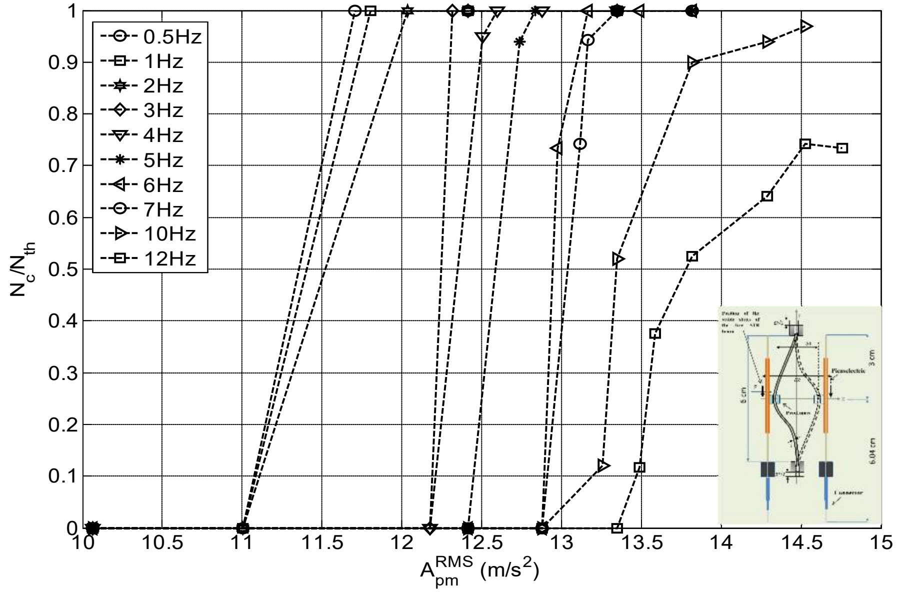

AR-STB-NLH

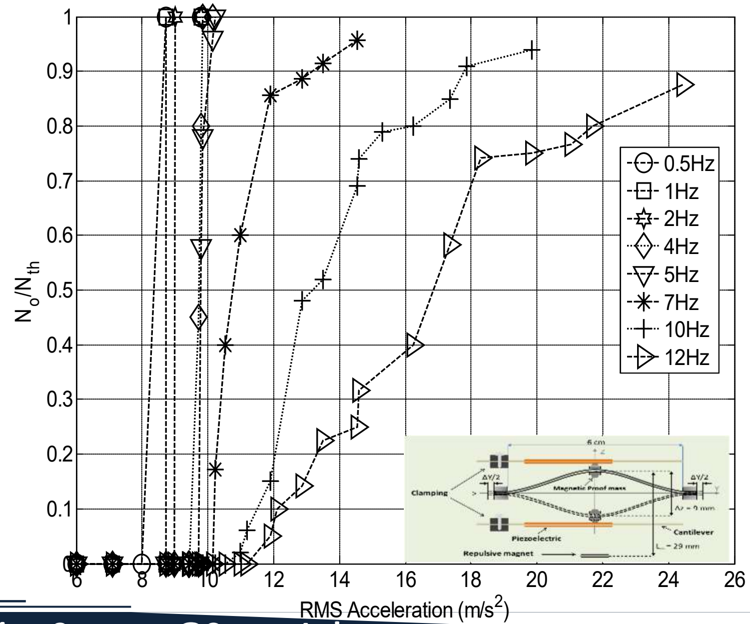

DIEEI – University of Catania, Italy

$$P_e = \frac{V_{RMS}^2}{R}\,(W)$$

where V_{RMS} is the RMS voltage measured across the load *R* (0.1 – 100 kΩ)

$$Efficiency: \eta = \frac{P_e}{P_m}$$

$$P_m = \frac{L}{t_s} = \frac{F * s}{t_s} = \frac{m * A_{RMS} * s}{t_s}$$

with

m = proof mass (4.11 g);

s = the distance the beam travels before switching (1 mm)

t_s= average switching time of the beam

A comparison between efficiencies

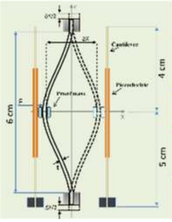

	PL-DP-STB-NLH				DP-STB-NLH			
f (Hz)	$A_{RMS}(m/s^2)$	P_m (W)	P_e (W)	η%	$A_{RMS}(m/s^2)$	P_m (W)	P_e (W)	η%
0.5	11.71	0.76e-3	29.33e-6	3.87	13.68	0.76e-3	26.68e-6	3.52
1	11.80	0.79e-3	55.79e-6	7.02	13.94	0.83e-3	49.05e-6	5.90
2	12.04	0.95e-3	103.85e-6	10.99	15.60	1.49e-3	115.80e-6	7.74
3	12.32	0.94e-3	117.92e-6	12.61	15.90	1.63e-3	158.71e-6	9.74
4	12.60	1.27e-3	203.26e-6	15.98	16.41	1.95e-3	226.29e-6	11.60
5	12.83	1.66e-3	273.85e-6	17.62	16.56	2.17e-3	271.00e-6	12.51

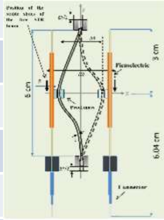

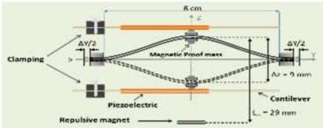

	AR-STB-NLH			
f (Hz)	A_{RMS} (m/s^2)	P_m (W)	P_e (W)	η%
0.5	8.71	0.54e-3	18.7e-6	3.5
1	8.74	0.54e-3	43.0e-6	8.0
2	8.82	0.78e-3	98.8e-6	12.7
4	9.93	1.55e-3	330.3e-6	21.3
5	10.22	1.76e-3	412.1e-6	23.5

Devices behaviour in case of a Band Limited Noise*

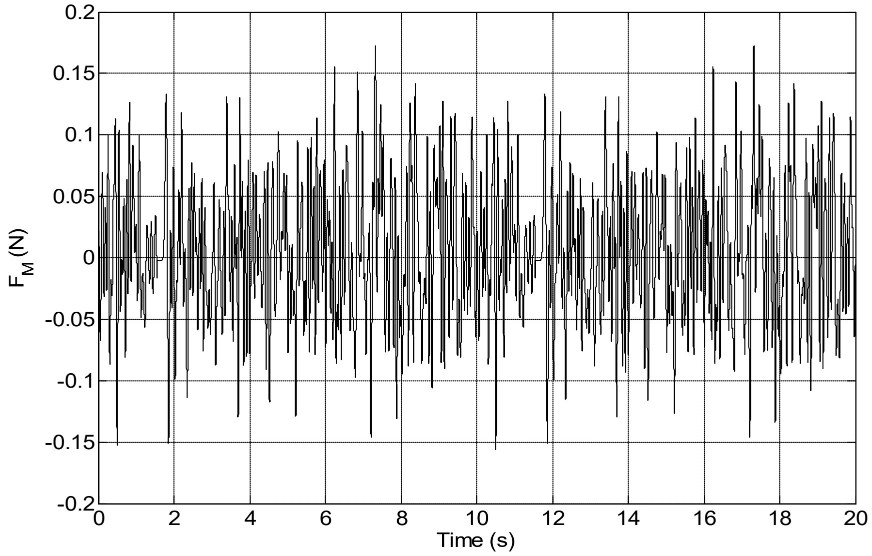

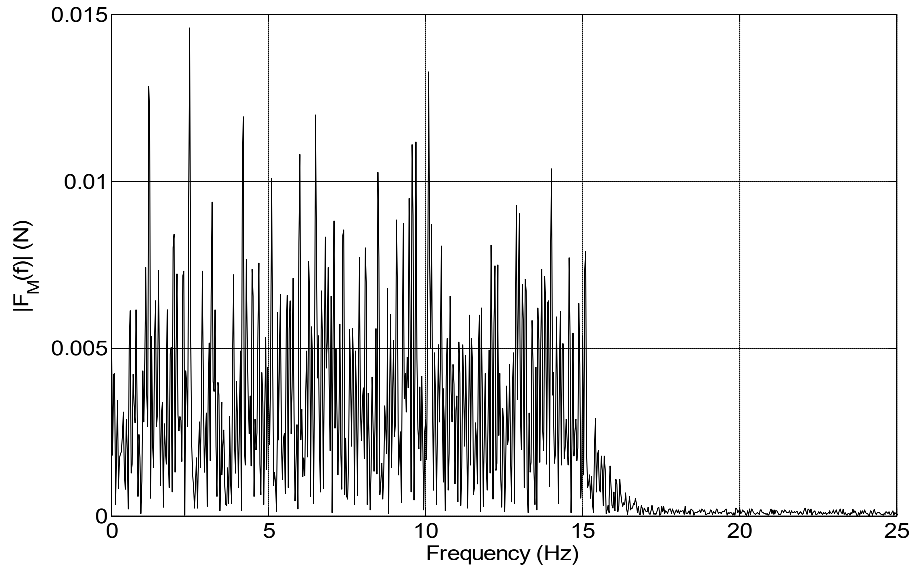

*Gaussian distributed pseudorandom pattern

THE DP-STB-NLH: observed switchings and piezoelectric output voltage

σ^2_{acc}= 31.25 m^2/s^4 Acc_max= 17.77 m/s^2

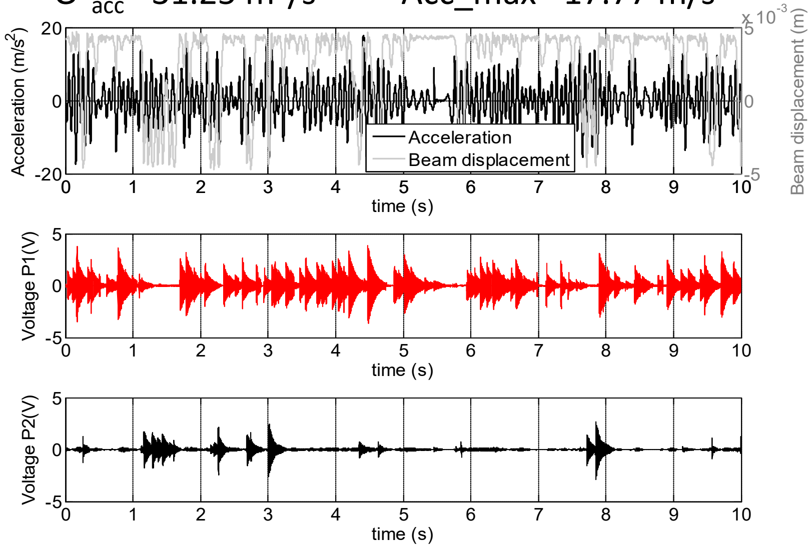

σ^2_{acc}= 39.92 m^2/s^4 Acc_max= 19.54 m/s^2

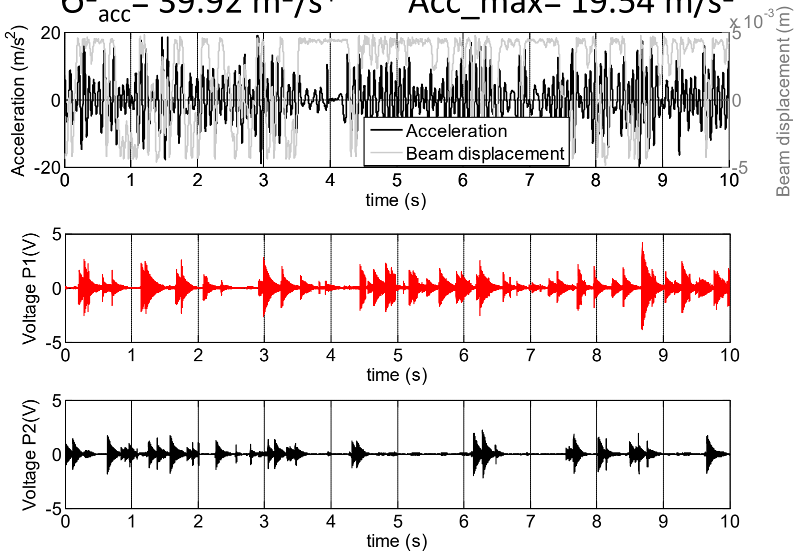

σ^2_{acc}= 53.52 m^2/s^4 Acc_max= 23.07 m/s^2

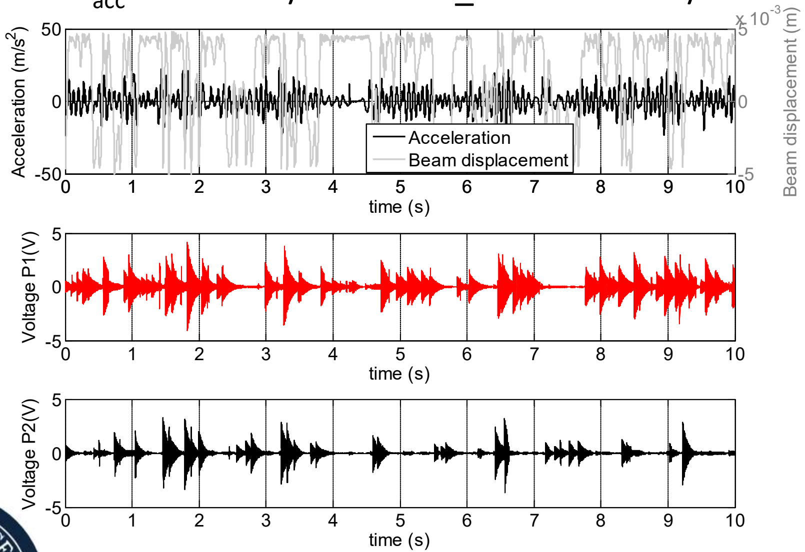

σ^2_{acc}= 78.50 m^2/s^4 Acc_max= 30.16 m/s^2

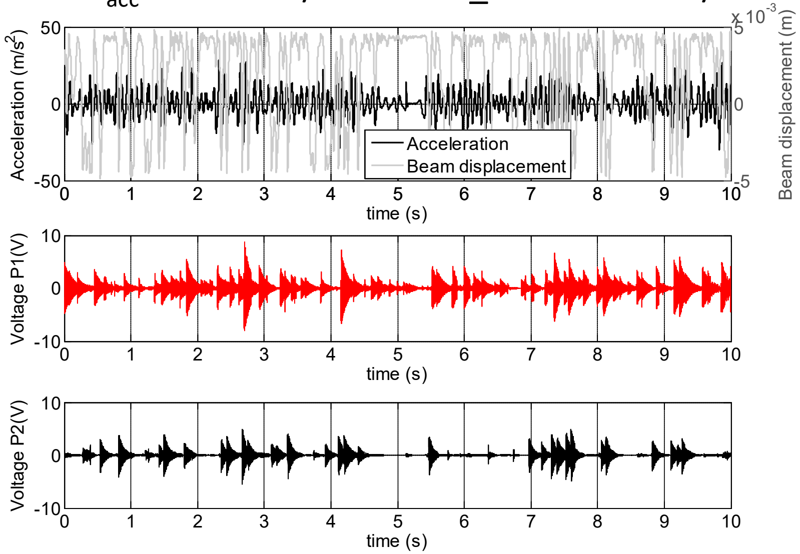

THE PL-DP-STB-NLH vs DP-STB-NLH

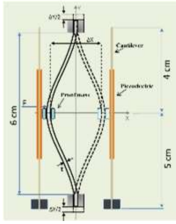

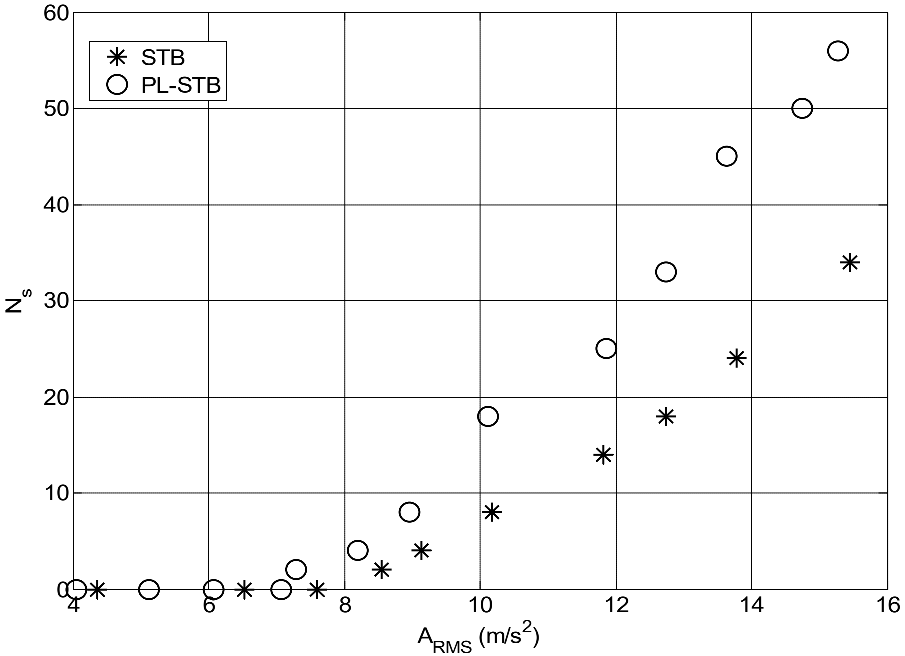

PL-DP-STB-NLH			
σ_A (m/s²)	P_m (W)	P_e (W)	η%
7.18	0.76e-3	4.23e-6	0.56
8.07	0.85e-3	16.25e-6	1.91
8.84	0.93e-3	27.21e-6	2.92
9.98	1.05e-3	65.56e-6	6.23
11.72	1.23e-3	123.87e-6	10.04
12.58	1.33e-3	160.98e-6	12.15
13.48	1.42e-3	187.50e-6	13.22
14.58	1.53e-3	225.07e-6	14.67
15.09	1.59e-3	248.63e-6	15.66

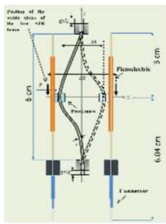

DP-STB-NLH			
σ_A (m/s²)	P_m (W)	P_e (W)	η%
8.42	0.89e-3	4.32e-6	0.49
9.00	0.95e-3	12.3e-6	1.29
10.03	1.06e-3	15.4e-6	1.46
11.65	1.23e-3	40.6e-6	3.30
12.56	1.33e-3	50.3e-6	3.80
13.60	1.43e-3	69.6e-6	4.86
15.25	1.61e-3	130e-6	8.03
17.07	1.80e-3	150e-6	8.23
18.88	1.99e-3	200e-6	10.14

THE AR-DP-STB-NLH

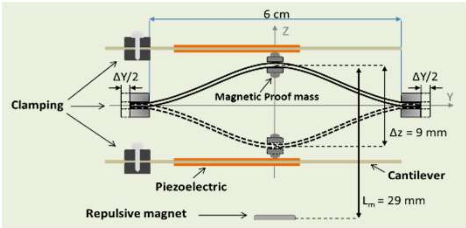

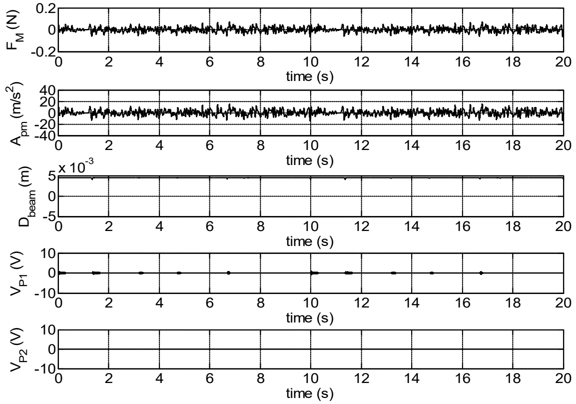

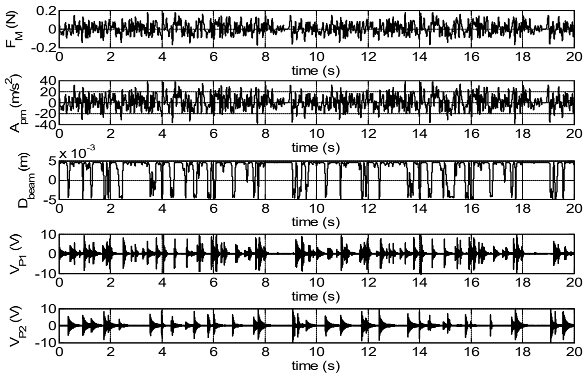

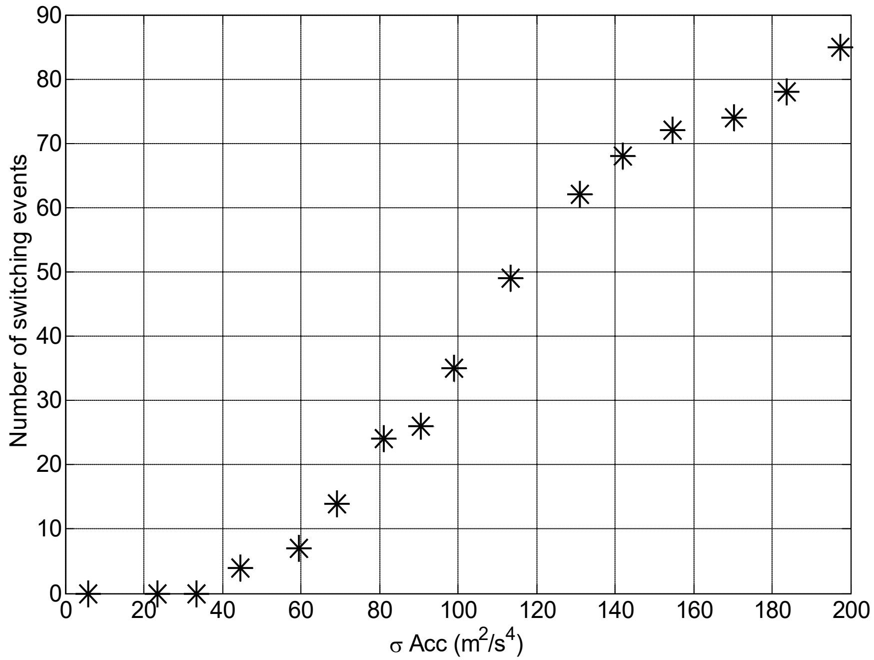

σ_{Acc} (m²/s⁴)	P_m (W)	P_e (W)	η%
59.52	8.29e-4	26.17e-6	3.16
113.4	1.15e-3	1.28e-4	11.2
197.3	1.51e-3	2.71e-4	17.88

Modeling

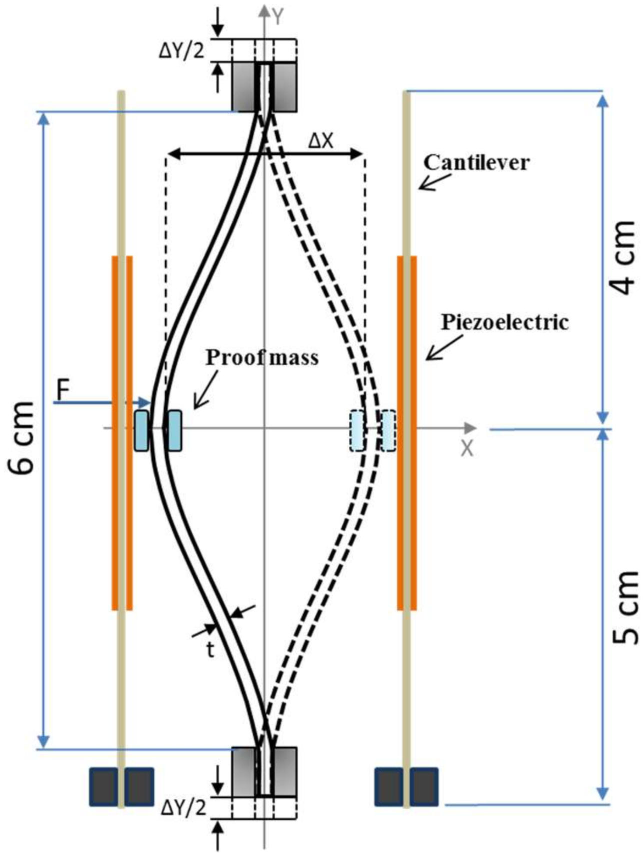
ΔY/2
Y
ΔX
Cantilever
4 cm
Piezoelectric
Proof mass
F
6 cm
X
5 cm
t
ΔY/2

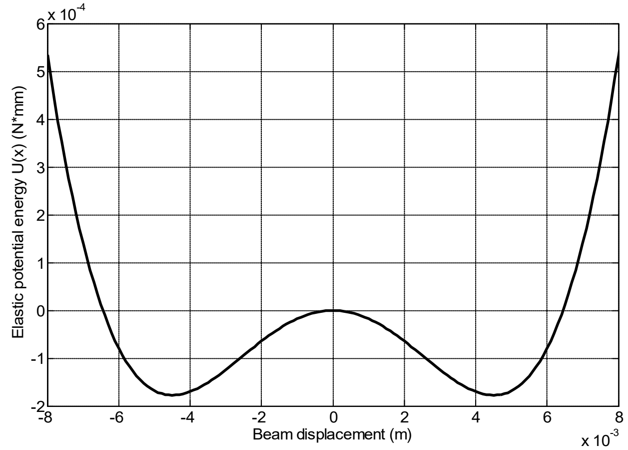
x 10^-4
Elastic potential energy U(x) (N*mm)
Beam displacement (m)
x 10^-3

MODELING OF THE DP-STB-NLH

$$m\ddot{x} + d\dot{x} - \Psi(x) = gF(t)$$

$$U(x) = \frac{cx^2}{2} - a\ln\cosh(bx)$$

$$\Psi(x) = -\frac{\partial U(x)}{\partial x} = -cx + ab\tanh(bx)$$

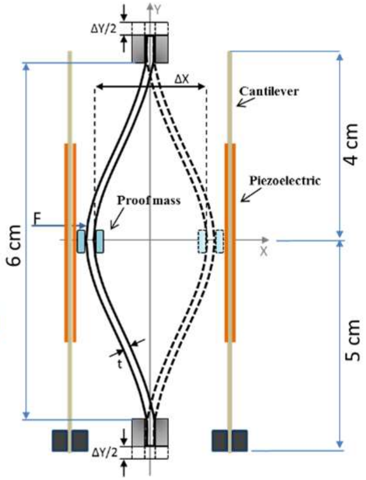

a, b, and *c* have been estimated by fitting the static behavior

a= 0.0561 N·m	*b*=100.8123 m^{-1}	*c*=533.6364 N/m

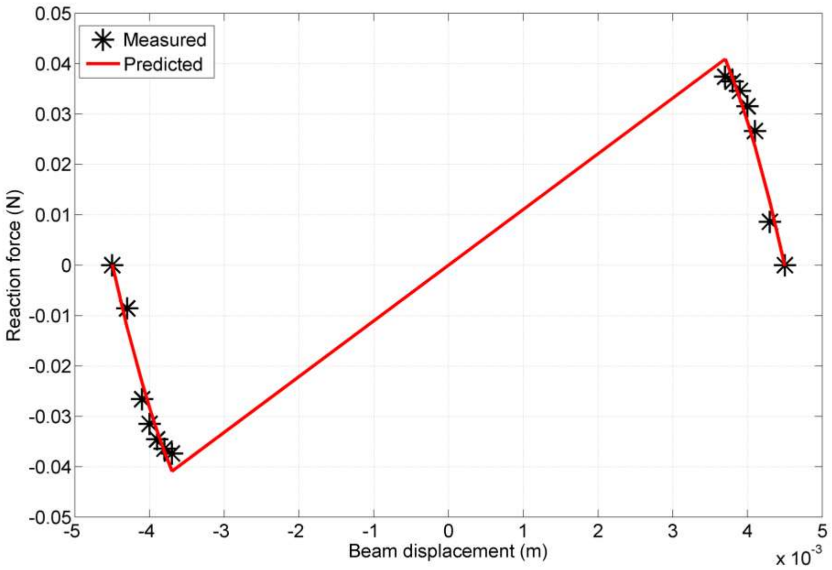

A comparison of the measured beam reaction force along the X-axis as a function of the displacement along the same axis and the predicted values by the proposed model

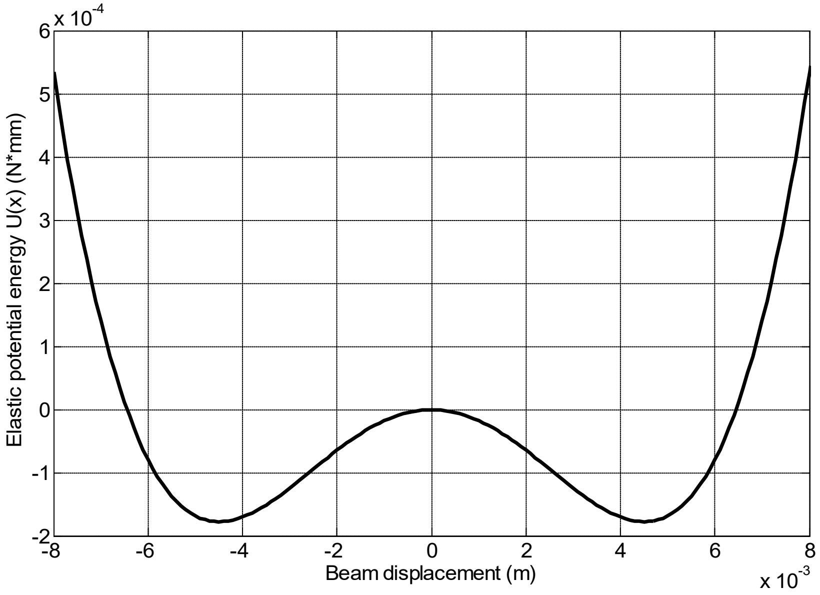

The elastic potential U(x) reconstructed by using the identified model parameters.

MODEL FITTING TO THE DYNAMIC MECHANICAL BEHAVIOR

$$m\ddot{x} + d\dot{x} - \Psi(x) = gF(t)$$

Parameters d and g, have been estimated by the Nelder-Mead optimization algorithm using the following minimization index:

$$J_N = \sqrt{\frac{\sum_i^n \left(\frac{N_{Meas} - N_{Pred}}{N_{Meas}} \right)^2}{n}}$$

N_{Meas} and N_{Pred} refer to the measured and predicted switchings of the bistable device

f=0.5Hz

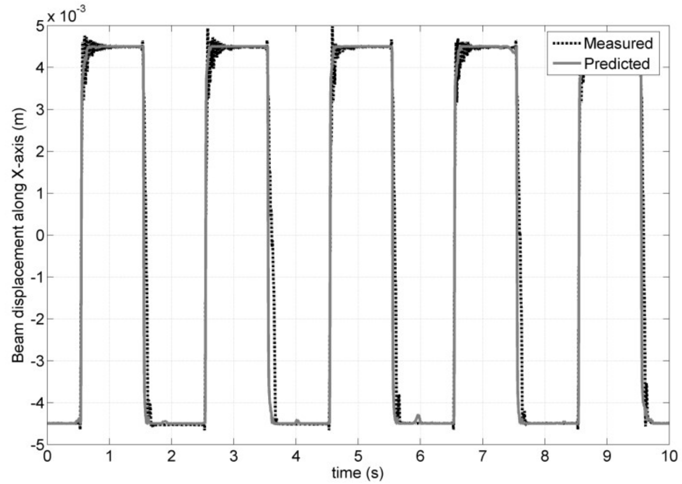

a= 0.0561 N·m	b=100.8123 m^{-1}	c=533.6364 N/m	d=0.7 N·s/m	g=-5.2

f=1Hz

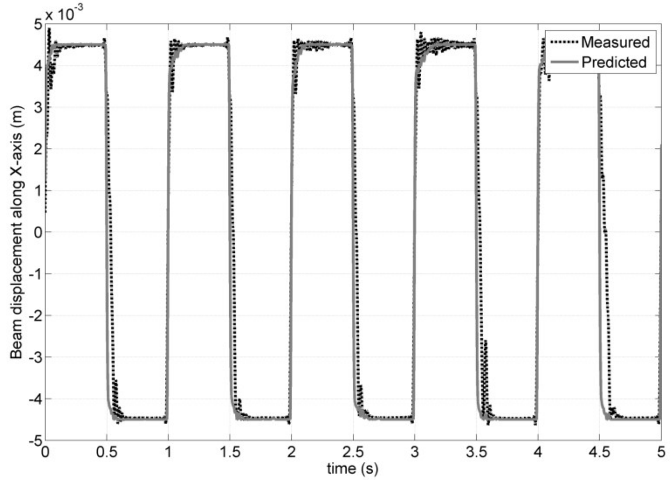

f=2Hz

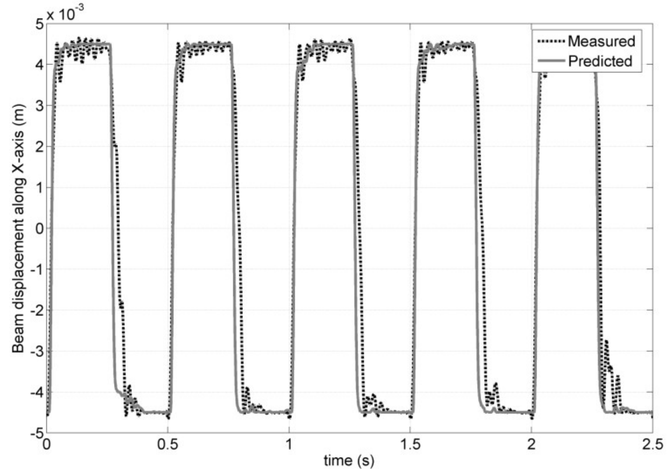

Model assessment in case of a Band Limited Noise input

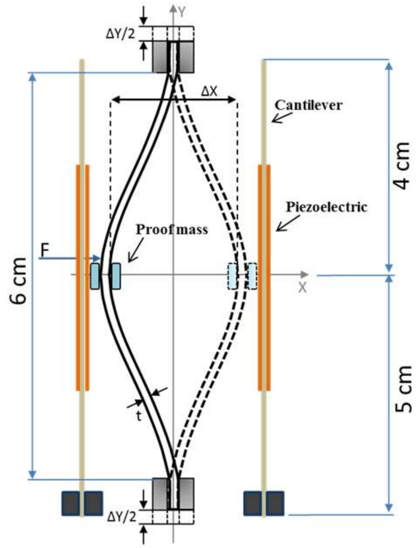

Model behaviour with a Band Limited Noise

$\sigma^2_{acc} = 3.81\ m^2/s^4$

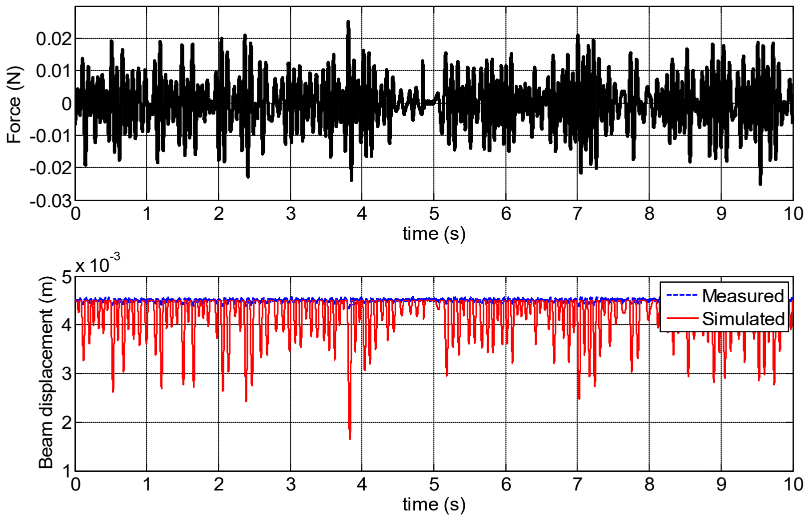

$\sigma^2_{acc} = 31.25\ m^2/s^4$

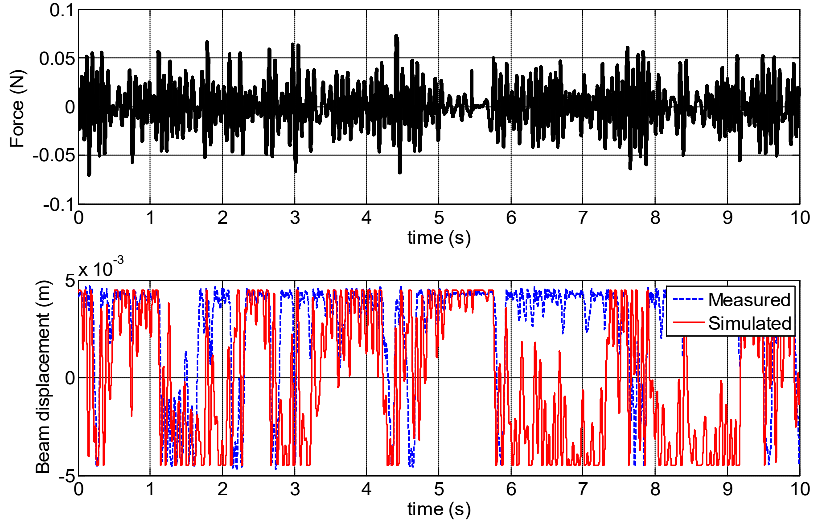

$\sigma^2_{acc} = 39.92\ m^2/s^4$

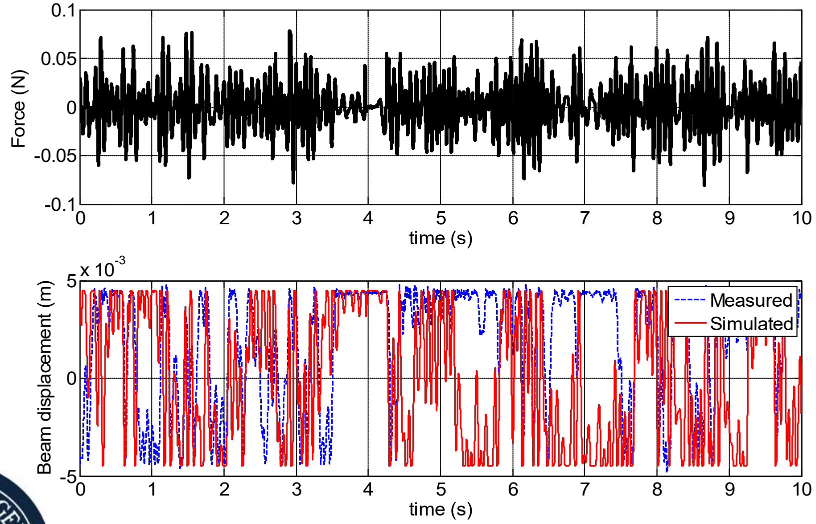

$\sigma^2_{acc} = 53.52\ m^2/s^4$

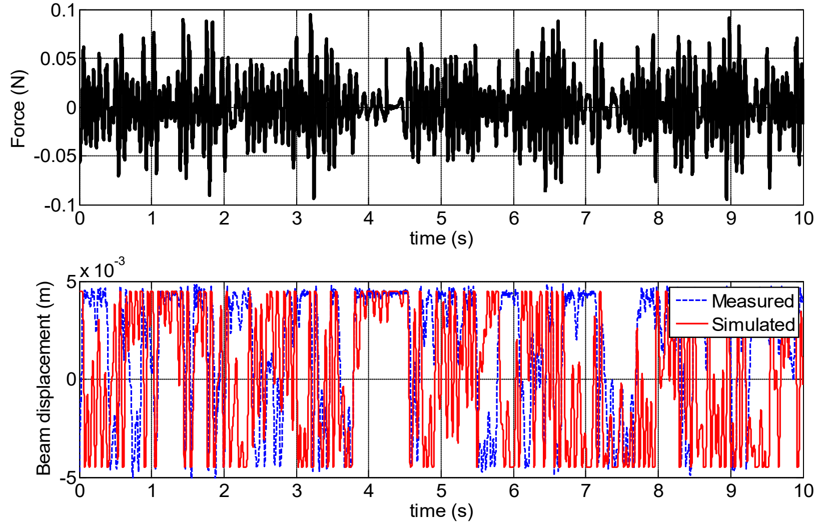

Model simulations with a Band Limited Noise

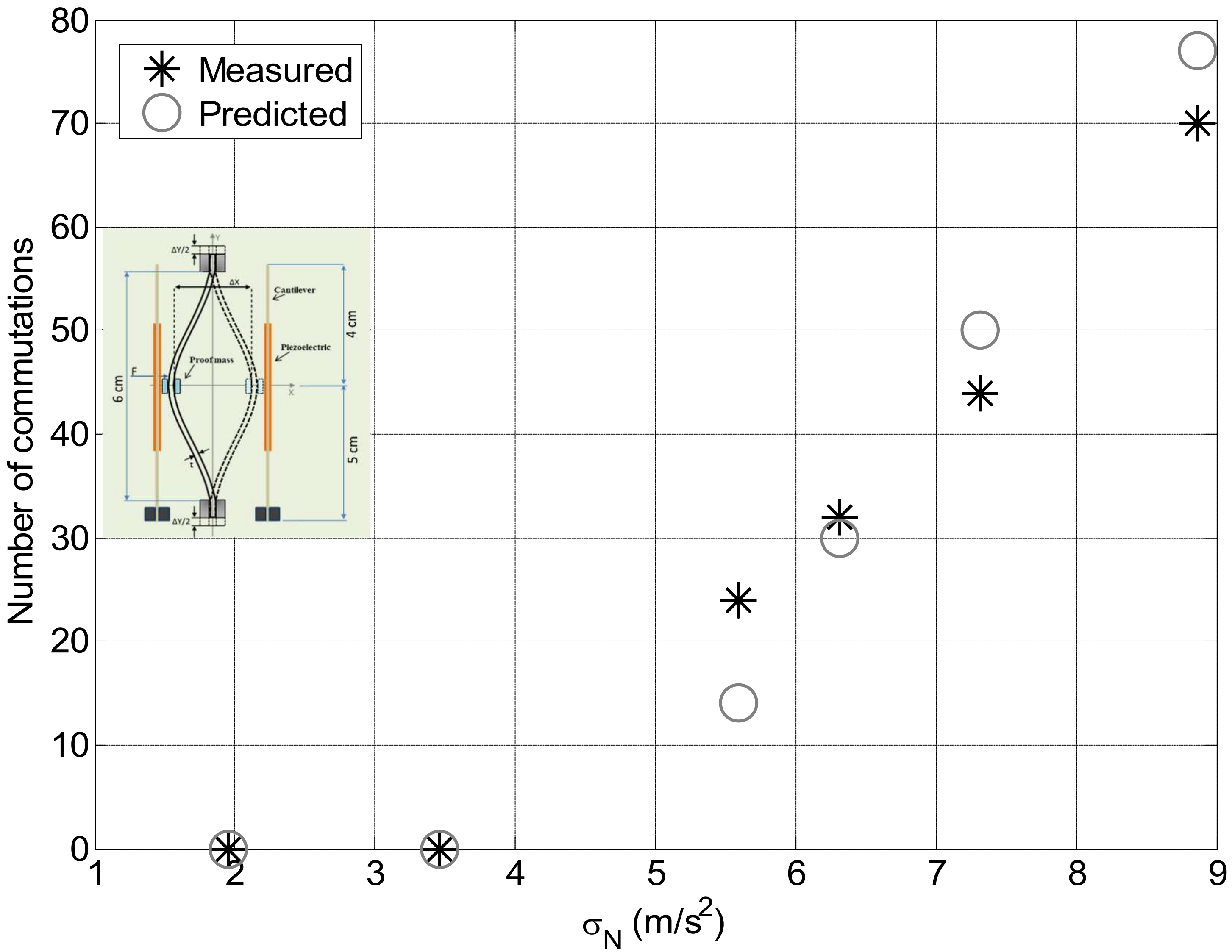

Number of switching events vs the standard deviation of the noise.

Simulations with a subthreshold deterministic signal with a superimposed Band Limited Noise

Subthreshold signal with a superimposed Band Limited Noise

$$F(t) = m(A\sin(\omega t) + n(t))$$

A and ω are the amplitude and the frequency of the deterministic signal, and *n(t)* is the band limited noise.

Examples in the case of a deterministic signal @1Hz (A= 13mN) and a noise signal limited at 100 Hz:

$\sigma_N{}^2 = 0.63\ m^2/s^4$ $\sigma_N{}^2 = 21.84\ m^2/s^4$ $\sigma_N{}^2 = 55.18\ m^2/s^4$

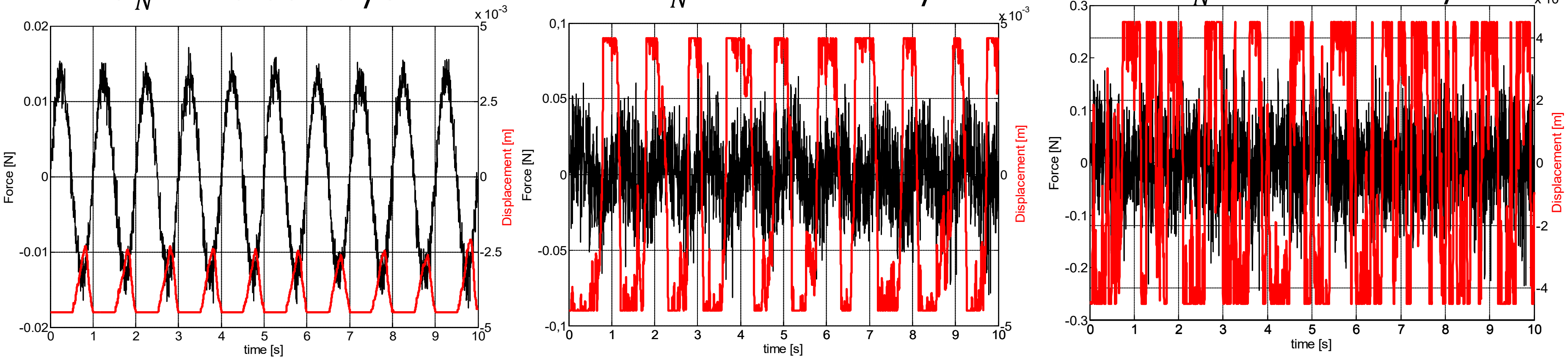

Number of switching events vs the variance of the noise

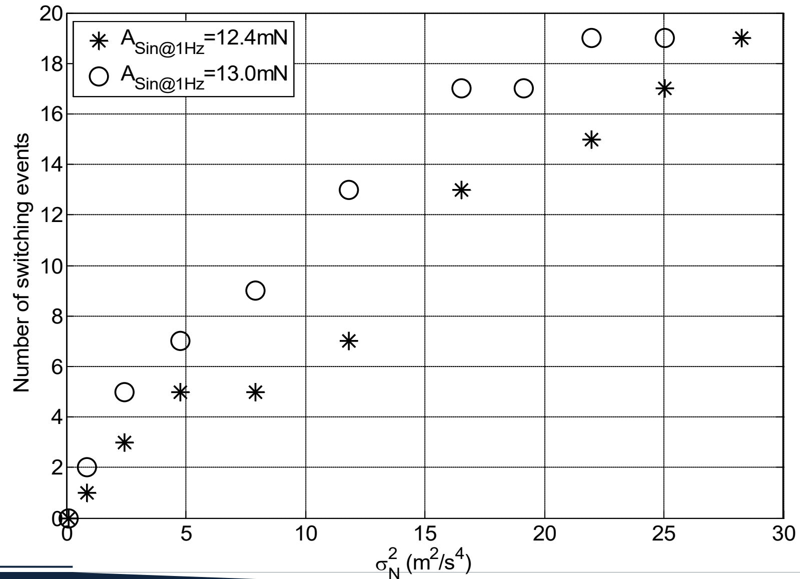

Subthreshold signal with a superimposed Band Limited Noise

$$SNR = \frac{S^{N+Sin}_{disp@1Hz}}{S^{N}_{disp@1Hz}}$$

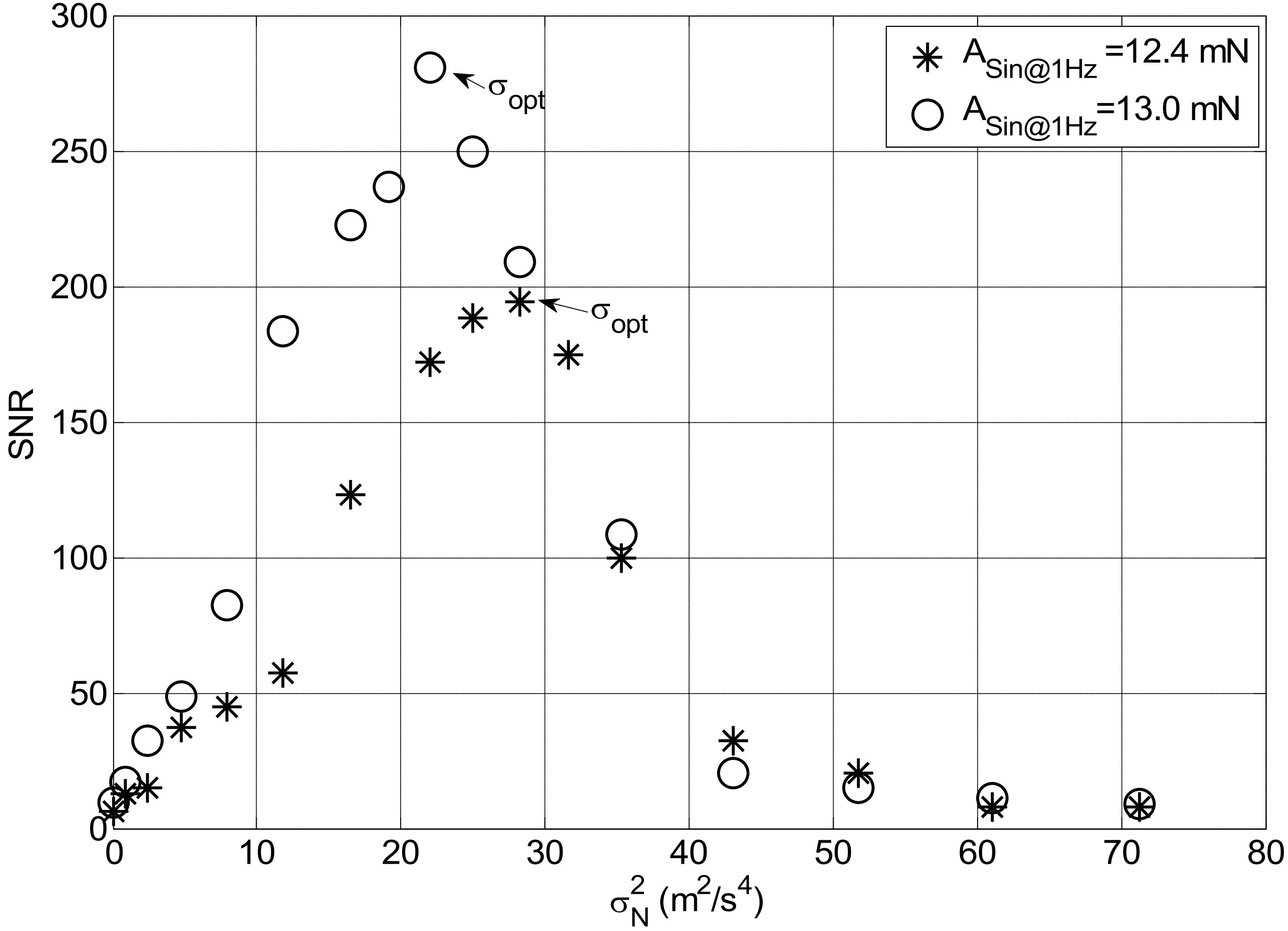

Signal-to-noise ratio vs the noise variance

OPEN PROBLEMS IN NOISE-ACTIVATED NLH

- *Development of a complete analytical model taking into account both mechanical and electrical behaviours*
- *Model assisted design*
- *Miniaturization and integration*
- *Experimental assessment of noise-deterministic driven behaviour*

Open problems of utilizing noise in energy harvesting systems

B. Andò, S. Baglio, A. R. Bulsara, V. Marletta

bruno.ando@unict.it

Sine: A= 12.4 mN, f= 1Hz

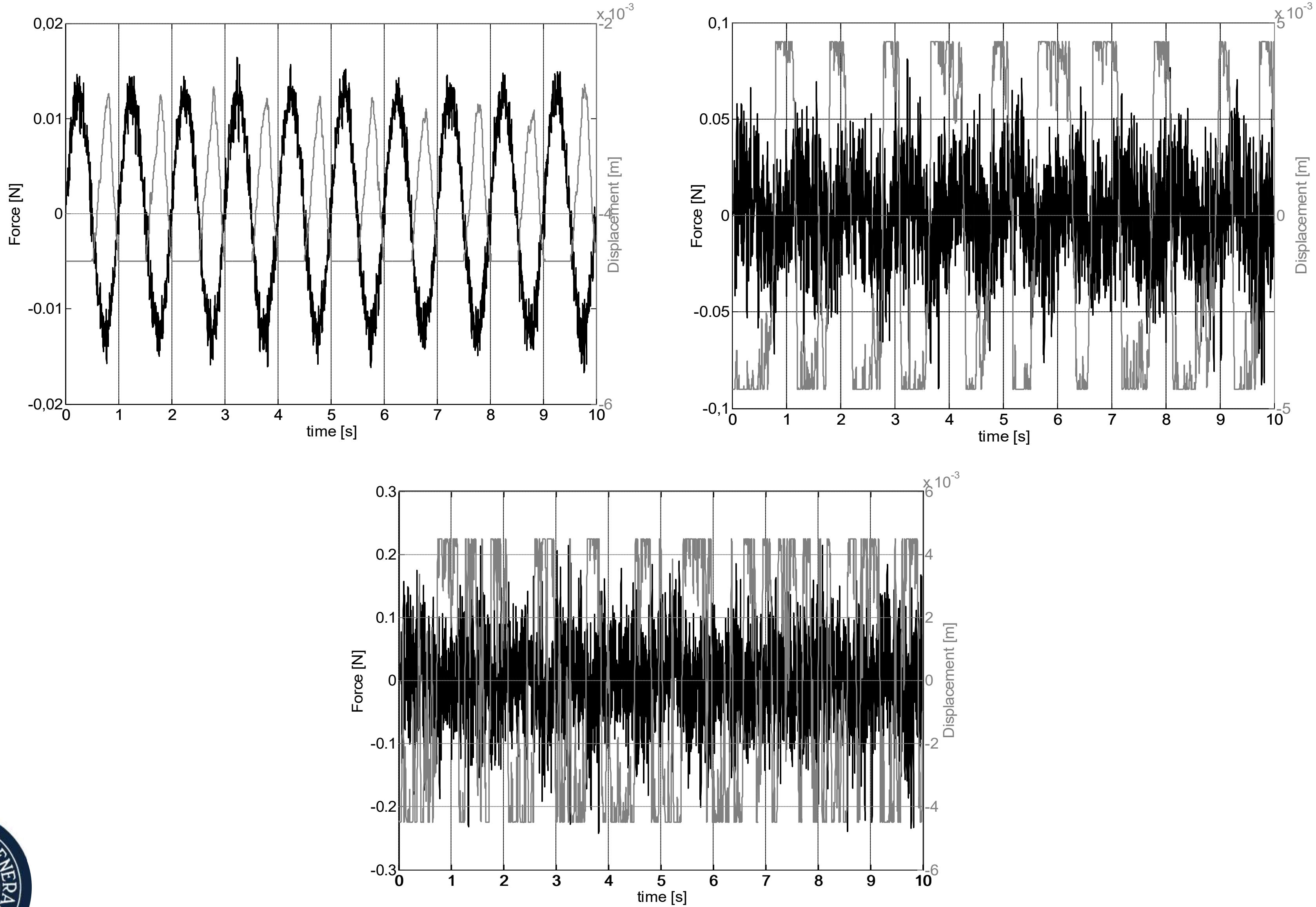

Electromagnetic vibration exciter

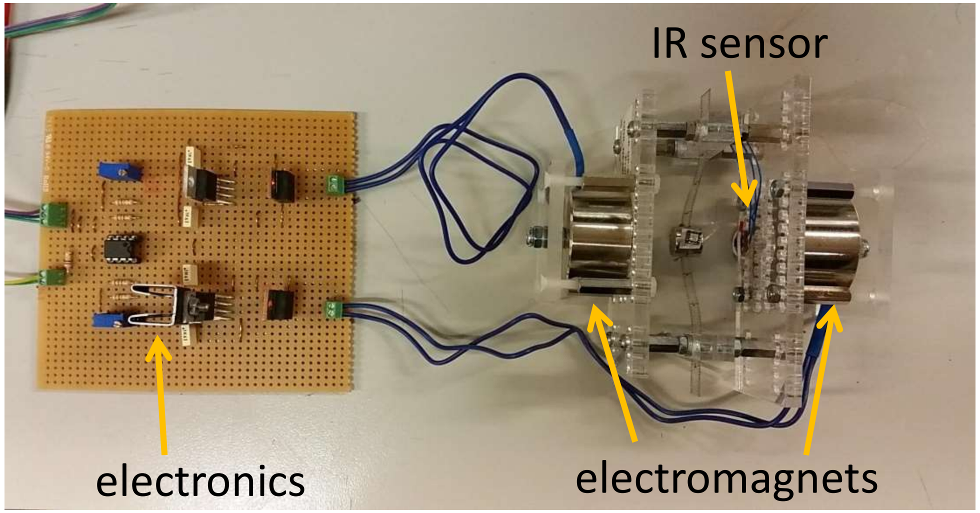

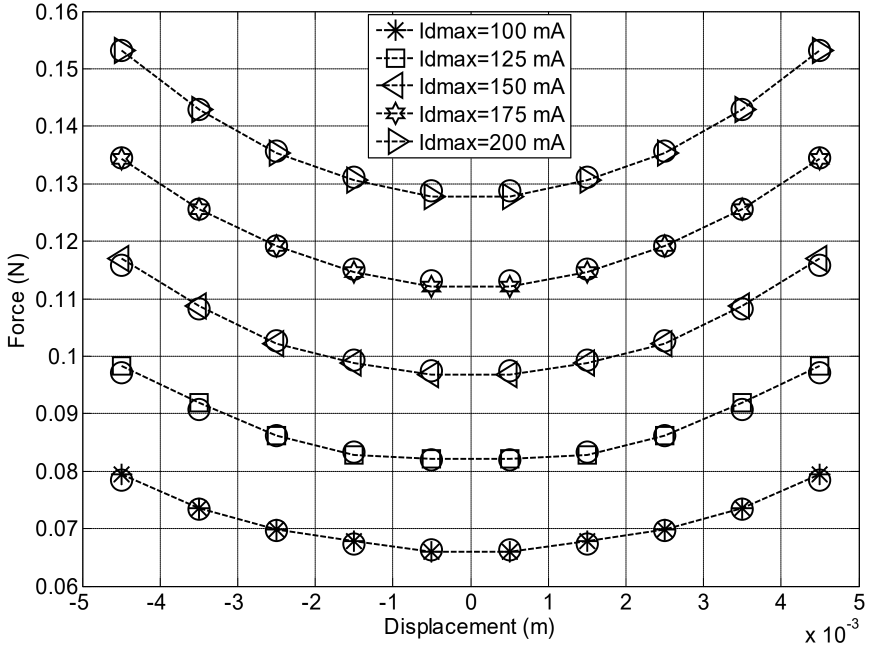

$$F_M = F_{EM1} + F_{EM2} = k \cdot I_d \cdot \left(\frac{L + x_1}{\sqrt{R^2 + (L + x_1)^2}} - \frac{x_1}{\sqrt{R^2 + x_1^2}} \right) + k \cdot I_d \cdot \left(\frac{L + x_2}{\sqrt{R^2 + (L + x_2)^2}} - \frac{x_2}{\sqrt{R^2 + x_2^2}} \right) + F_x$$

percentage root mean square error: $$J_{stat}\% = 100 \cdot \sum_{i=1}^{m} \left(\sqrt{\frac{\sum_{j=1}^{n} \left(\frac{F_M^{meas} - F_M^{sim}}{F_M^{meas}} \right)^2}{n}} \right)$$

k = 26.152 m*T

F_x = 0.0037 N

CHARACTERIZATION OF THE AR-DP-STB-NLH BY THE NEW SETUP

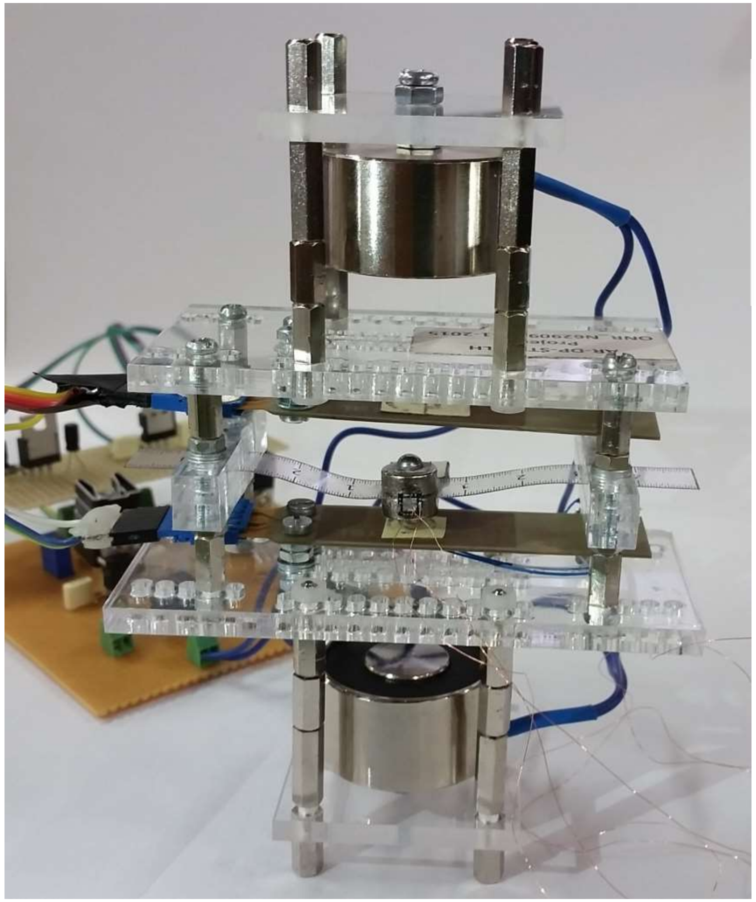

The proof mass on the beam is composed by **two** neodymium permanent magnets S-10-04-N (with a total weight F_l = 4.6 g) and 2 hemispherical inox steel parts to improve the impact on the piezoelectric beams

Material	NdFeB
Diameter	10 mm
Height	4 mm
Direction of magnetisation	axial (parallel to height)
Coating	Nickel-plated (Ni-Cu-Ni)
Magnetisation	N42
strength	approx. 2 kg (approx. 19,6 N)

The repulsive magnet is a neodymium permanent magnets S-08-01-N

Material	NdFeB
Diameter	10 mm
Height	1 mm
Direction of magnetisation	axial (parallel to height)
Coating	Nickel-plated (Ni-Cu-Ni)
Magnetisation	N35
strength	approx. 500 g (approx. 4,9 N)

EXPERIMENTAL CHARACTERIZATION OF THE AR-DP-STB-NLH

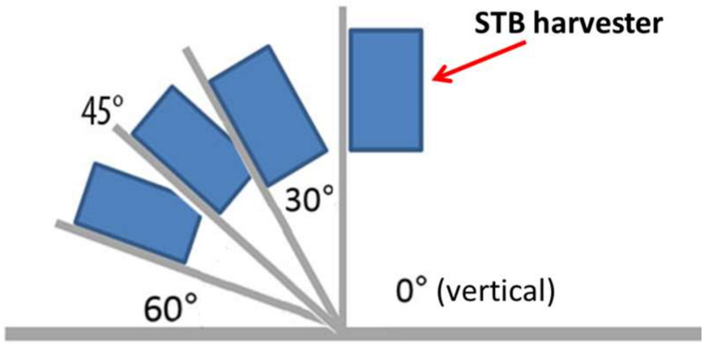

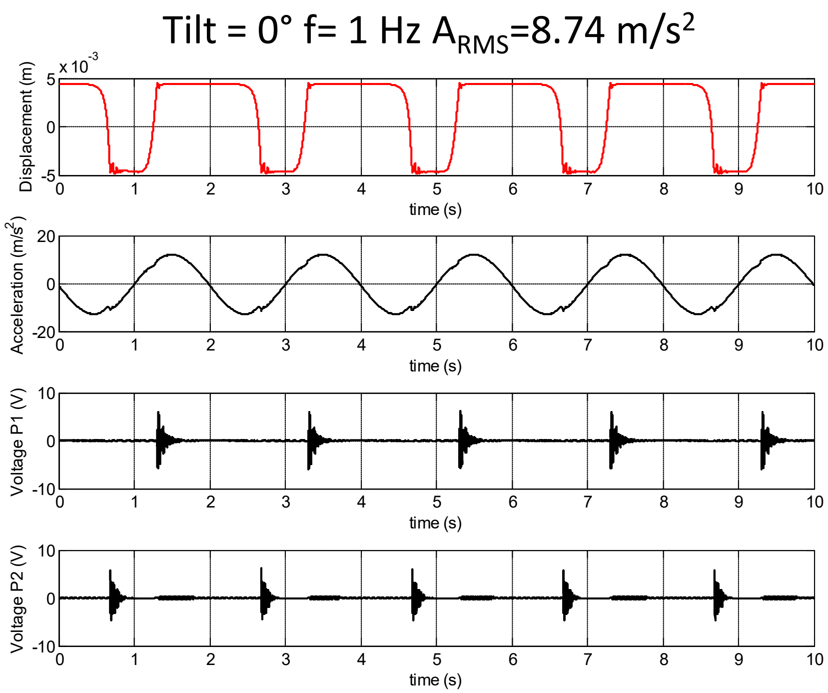

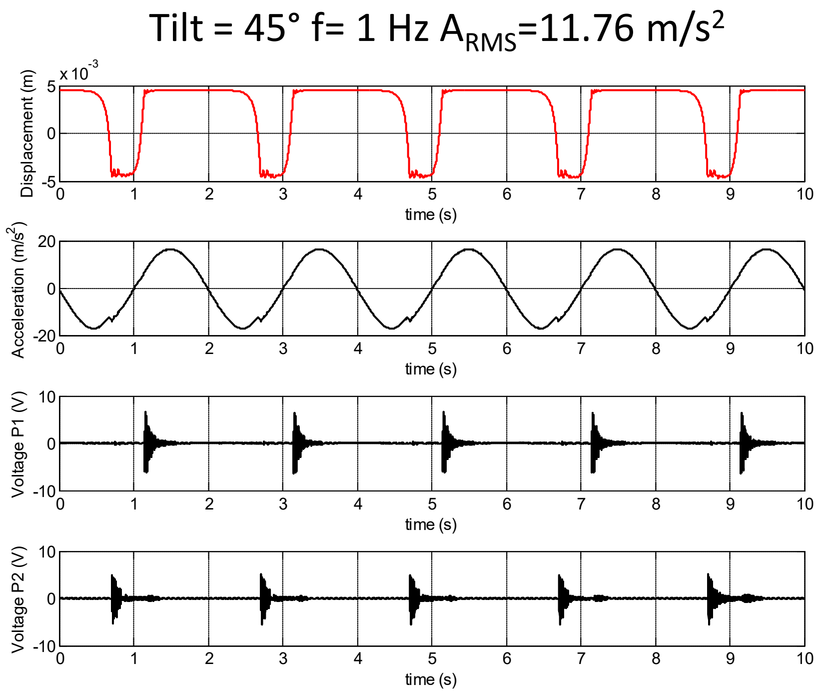

Examples of observed signals in case of the minimum acceleration assuring the maximum switching rate @ 1Hz

The values of the minimum RMS acceleration, A_{RMS}, assuring the maximum switching rate for each frequency and tilt configuration, in the case of the repulsive permanent magnet placed underneath.

		Tilt (°)			
		0	30	45	60
Frequency (Hz)	0.5	8.72 m/s²	9.71 m/s²	10.98 m/s²	13.86 m/s²
	1	8.73 m/s²	9.73 m/s²	11.2 m/s²	13.96 m/s²
	2	9.01 m/s²	9.85 m/s²	11.76 m/s²	15.21 m/s²
	4	9.84 m/s²	10.94 m/s²	13.24 m/s²	15.91 m/s²
	5	10.22 m/s²	12.85 m/s²	14.27 m/s²	17.88 m/s²

The values of the minimum RMS acceleration, A_{RMS}, assuring the maximum switching rate for each frequency and tilt configuration, in the case without repulsive permanent magnet placed underneath.

		Tilt (°)			
		0	30	45	60
Frequency (Hz)	0.5	16.73 m/s²	16.41 m/s²	15.78 m/s²	14.55 m/s²
	1	17.37 m/s²	16.52 m/s²	16.15 m/s²	14.57 m/s²
	2	17.37 m/s²	16.95 m/s²	16.15 m/s²	14.78 m/s²
	4	18.64 m/s²	18.40 m/s²	16.94 m/s²	16.13 m/s²
	5	21.03 m/s²	20.01 m/s²	19.42 m/s²	18.64 m/s²

THE PL-DP-STB-NLH

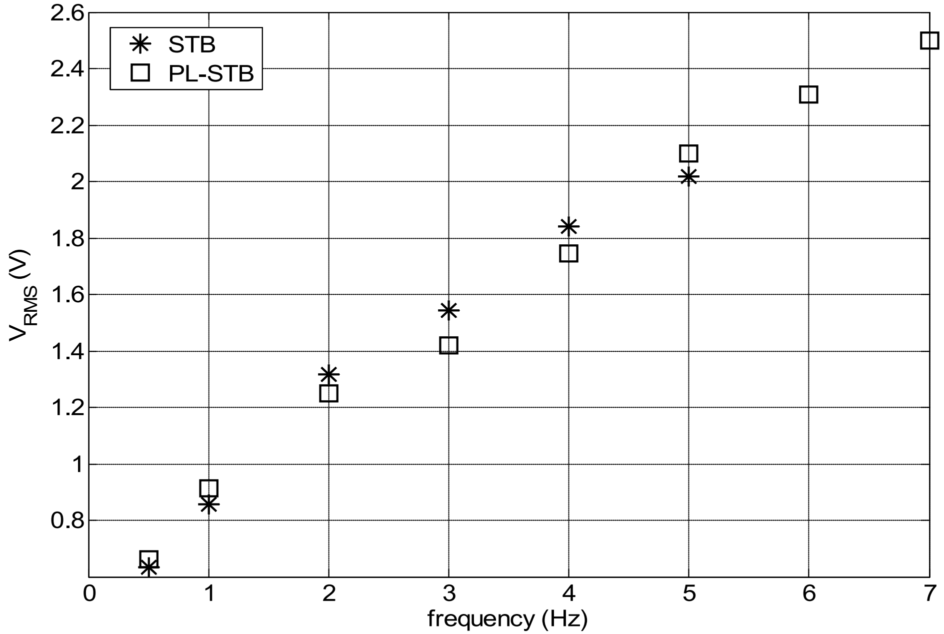

EXPERIMENTAL CHARACTERIZATION OF THE AR-DP-STB-NLH: Tilt = 0°

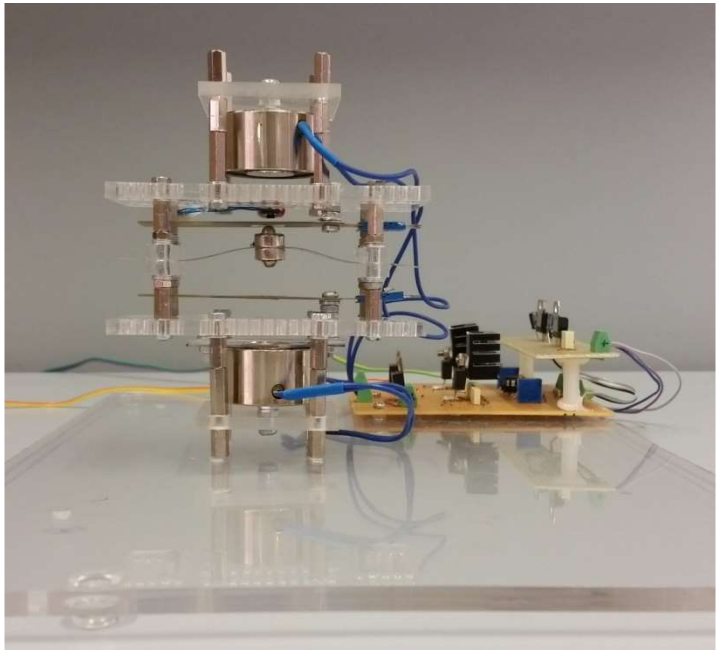

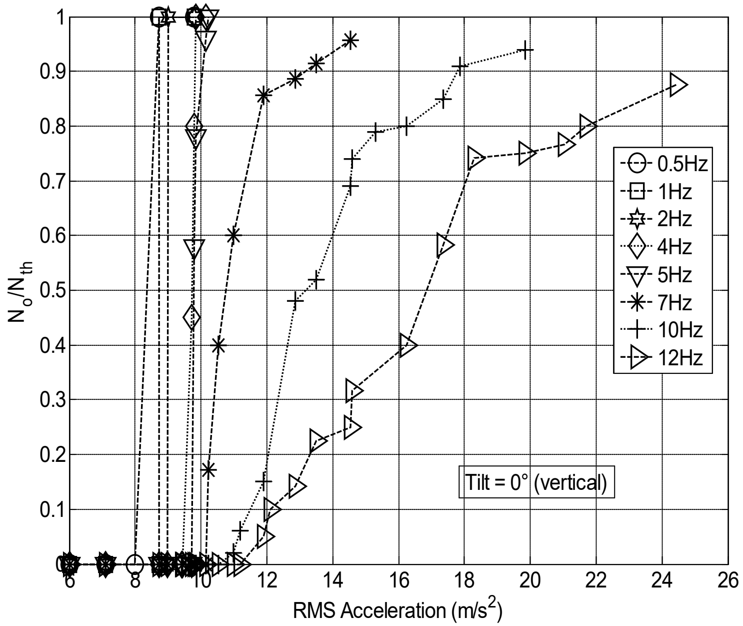

Normalized number of complete switches vs the RMS acceleration

THE ENERGY CONVERSION EFFICIENCY

f (Hz)	a_{RMS} (m/s^2)	P_m (W)	P_e (W)	η%
0.5	8.71	0.54e-3	1.87e-5	3.5
1	8.74	0.54e-3	4.30e-5	8.0
2	8.82	0.78e-3	9.88e-5	12.7
4	9.93	1.55e-3	33.03e-5	21.3
5	10.22	1.76e-3	41.21e-5	23.5

The electrical power produced by the DP-NLH device as been evaluated as:

$$V_{RMS}^2 / R$$

where V_{RMS} is the RMS voltage measured across the load R = 15 kΩ assuring the optimal power transfer.

The performance of the STB harvester has been evaluated by estimating the power conversion efficiency: $\eta\% = \frac{P_e}{P_m} 100$ where, P_e and P_m denote the electrical and mechanical power, respectively.

ΔY=1mm (precompression)
ΔX=9mm (distance between stable states)

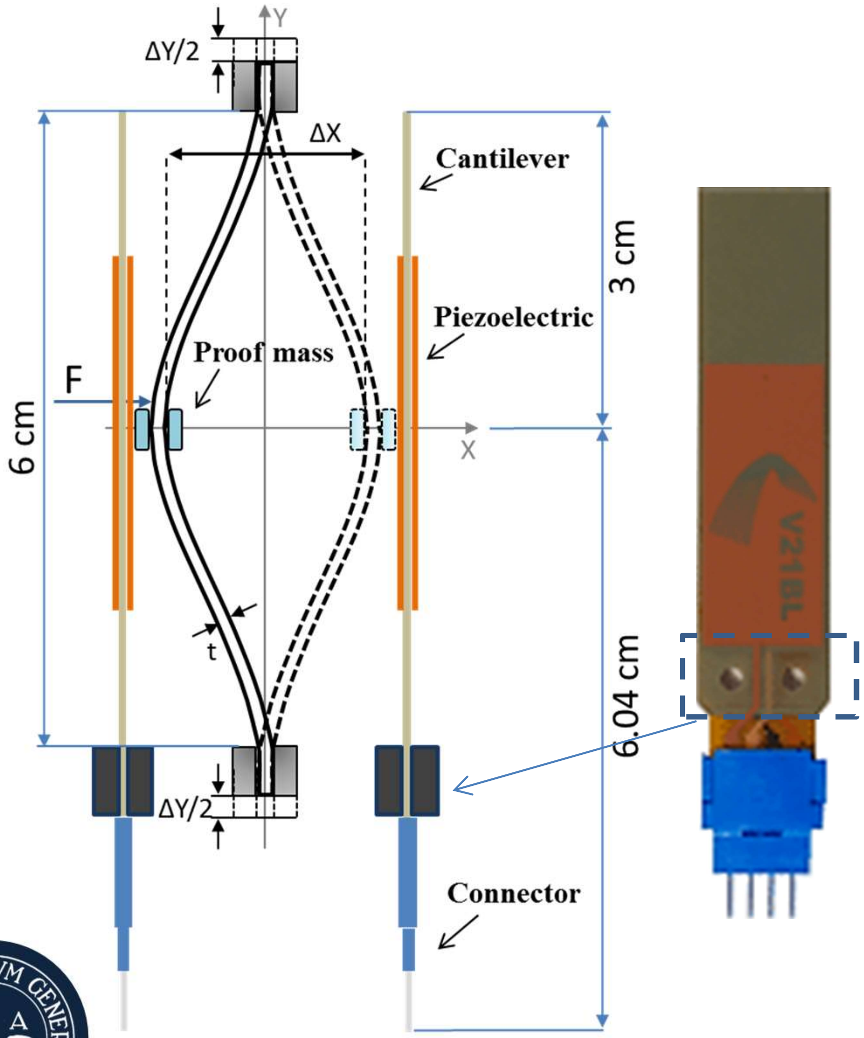

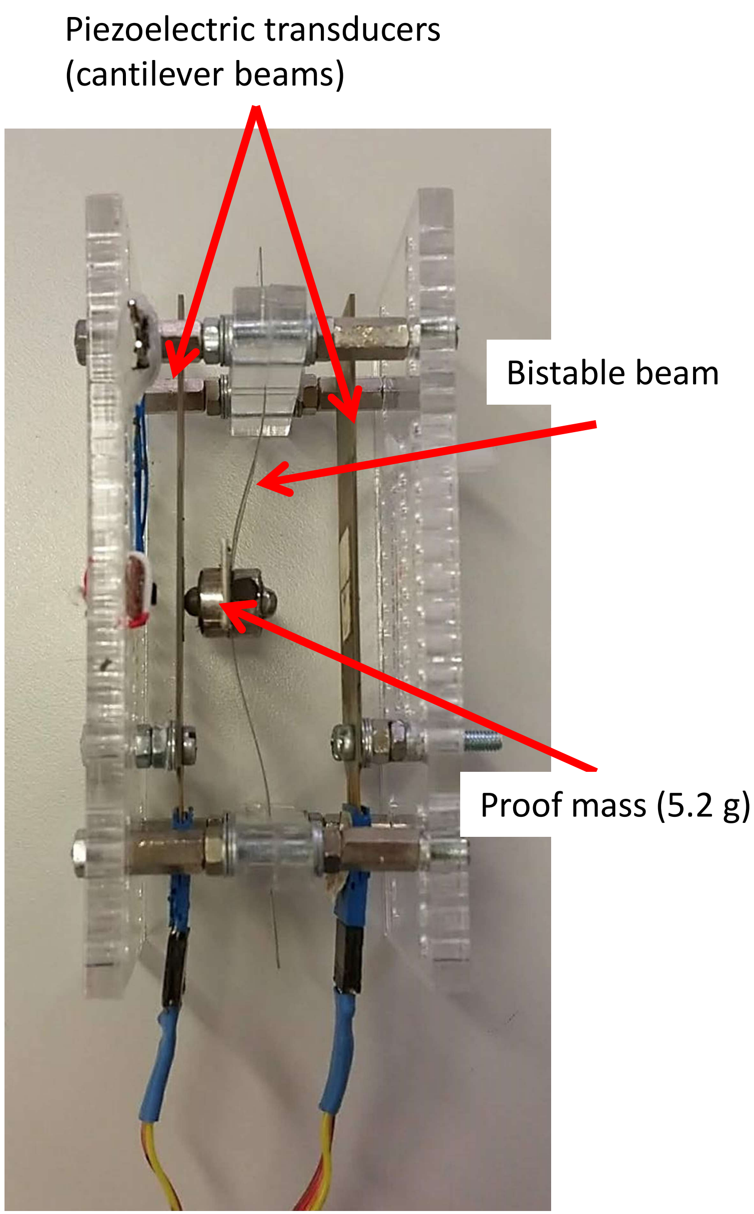

THE DP-STB-NLH: Electrical efficiency evaluation

$A_{RMS\ (m/s^2)}$	V_{RMS} (V)	P_m (W)	P_e (W)	η%
5.59	0.74	0.58e-03	54.07e-06	9.27
6.32	0.79	0.66e-03	62.00e-06	9.40
7.32	1.02	0.76e-03	104.80e-06	13.73
8.86	1.27	0.92e-03	160.00e-06	17.31

P_m= mechanical power evaluated as $P_m = \frac{L}{t_s} = \frac{F * s}{t_s} = \frac{m * A_{RMS} * s}{t_s}$

with

t_s= 0.039 average switching time of the beam

m = proof mass (4.11 g);

s = the distance the beam travels before switching (1 mm)

P_e = electrical power evaluated as $P_e = \frac{V_{RMS}^2}{R_{load}}$

$\eta = \frac{P_e}{P_m}$ is the electrical efficiency of the harvester

THE PL-DP-STB-NLH

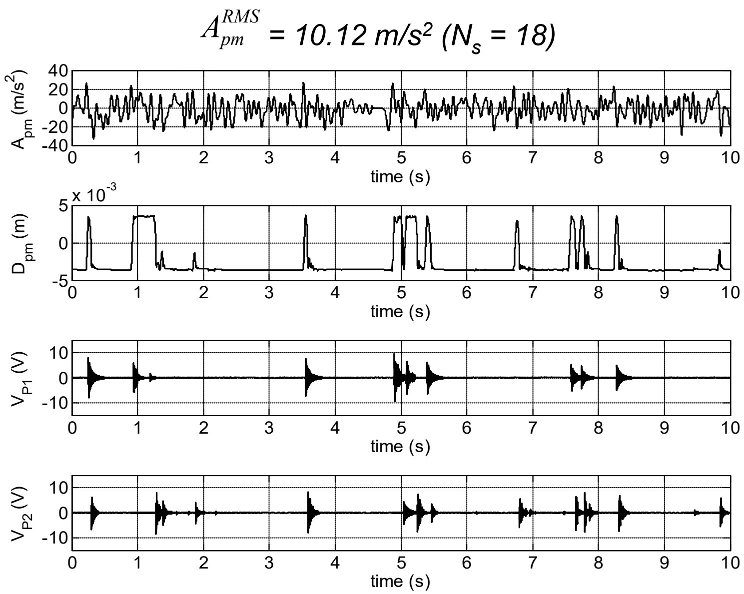

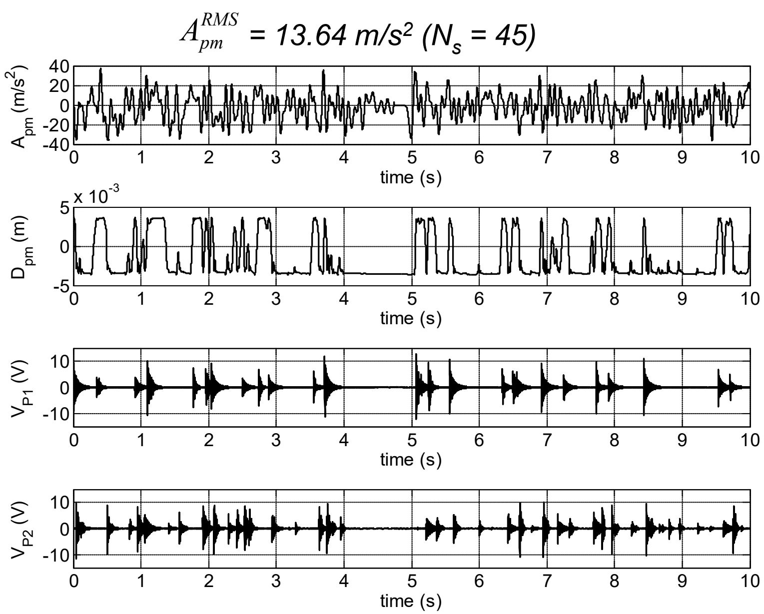

Model simulations with a Band Limited Noise

Acc_RMS= 8.86 m/s²

σ_{acc}= 78.56 m/s²